# Functional Modification of Anchote Starch: Study on the Effect of Gum Arabic, Polyvinylpyrrolidone, and Boric acid on an acetylated starch Adhesive Performance

Teketel Alemu Anshebo

A Thesis Submitted to

The Department of Chemical Engineering

School of Mechanical, Chemical and Materials Engineering

Presented in Partial Fulfillment of the Requirement of the Degree of Master's in Chemical Engineering (Specialization in Process Engineering)

Office of Graduate Studies

Adama Science and Technology University

Adama, Ethiopia

August, 2021

# Functional Modification of Anchote starch: Study on the Effect of Gum Arabic, Polyvinylpyrrolidone, and Boric acid on an acetylated starch Adhesive Performance

Teketel Alemu Anshebo

**Advisors**

Tatek Temesgen Terfasa (Ph.D.)

Melaku Tesfaye Alemea (Ph.D.)

A Thesis Submitted to

The Department of Chemical Engineering
School of Mechanical, Chemical, and Material Engineering
Presented in Partial Fulfillment of the Requirement of the Degree of Master's in Chemical Engineering (Specialization in Process Engineering)

Office of Graduate Studies
Adama Science and Technology University

Adama, Ethiopia

August, 2021

# APPROVAL SHEET

We hereby certify that the recommendations and suggestions made by the board of examiners are appropriately incorporated into the final version of the dissertation entitled **"Functional Modification of Anchote starch: Study on the Effect of Gum arabic, Polyvinylpyrrolidone, and Boric acid on an acetylated starch Adhesive Performance**" by Teketel Alemu Anshebo

| | | |
|---|---|---|
| Tatek Temesgen Terfasa (Ph.D.) | _____ | _____ |
| Major Advisor | Signature | Date |
| Melaku Tesfaye Alemea (Ph.D.) | _____ | _____ |
| Co-Advisor | Signature | Date |

We, the undersigned, members of the Board of Examiners of the thesis by Teketel Alemu Anshebo have read and evaluated the thesis entitled "**Functional Modification of Anchote starch: Study on the Effect of Gum arabic, Polyvinylpyrrolidone, and Boric acid on an acetylated starch Adhesive Performance**" and examined the candidate during the open defense. This is, therefore, to certify that the thesis is accepted for partial fulfillment of the requirement of the degree of Master of Science in Chemical Engineering (Specialization in Process Engineering).

| | | |
|---|---|---|
| _____ | _____ | _____ |
| Chairperson | Signature | Date |
| _____ | _____ | _____ |
| Internal Examiner | Signature | Date |
| _____ | _____ | _____ |
| Eternal Examiner | Signature | Date |

Finally, approval and acceptance of the dissertation is contingent upon submission of its final copy to the Office of Postgraduate Studies (OPGS) through the candidate's Department Graduate Council (DGC) and School Graduate Committee (SGC).

| | | |
|---|---|---|
| _____ | _____ | _____ |
| Department Head | Signature | Date |
| _____ | _____ | _____ |
| School Dean | Signature | Date |
| _____ | _____ | _____ |
| Postgraduate Studies, Dean | Signature | Date |

# DECLARATION

I hereby declare that this Master Thesis entitled "**Functional Modification of Anchote starch: Study on the Effect of Gum Arabic, Polyvinylpyrrolidone, and boric acid on an acetylated starch Adhesive Performance**" is my original work and has not been submitted for the award of any academic degree, diploma or certificate in any other university. All sources of materials used for this thesis have been duly acknowledged through appropriate citations.

| Teketel Alemu Anshebo | _____ | _____ |
|---|---|---|
| Name of student | Signature | Date |

We, the advisors of this thesis, hereby certify that we have read the revised version of the thesis entitled "**Functional Modification of Anchote starch: Study on the Effect of Gum Arabic, Polyvinylpyrrolidone, and boric acid on an acetylated starch Adhesive Performance**" prepared under our guidance by Teketel Alemu Anshebo submitted in partial fulfillment of the requirements for the degree of Mater's of Science in Chemical Engineering (Specialization in Process Engineering). Therefore, we recommend the submission of the revised version of the thesis to the department following the applicable procedures.

| Tatek Temesgen Terfasa (Ph.D.) | _____ | _____ |
|---|---|---|
| Major Advisors | Signature | Date |
| Melaku Tesfaye Alemea (Ph.D.) | _____ | _____ |
| Co-Advisor | Signature | Date |

# ACKNOWLEDGMENT

First, I would like to express my heartfelt thanks to Almighty **God** for giving me the strength, dedication, inspiration, and wisdom to achieve and complete this MSc. program.
I would like to express my gratitude to my main advisors Tatek Temesgen (Ph.D.) and Co-advisor Melaku Tesfaye (Ph.D.) for their support, guidance and valuable criticisms, inspiration, and endless encouragement. This thesis would not have been accomplished without their outstanding supervision, scientific knowledge, and experience.

Also, I would like to express my deepest thank to the Department of chemical engineering for countless support and my great appreciation goes to all laboratory staff of the department for patient full support. Additionally, I want to express my genuine and regards to all my classmates and friends at ASTU for their contribution to accomplish thesis work. Moreover, I would like to express my sincere thanks to Adama Science and Technology University for their financial grant (Grant ASTU/SM-R/123/19).

Finally, I would like to give heartfelt thanks with the deepest gratefulness to my family for offering enormous and uncountable support throughout my entire life.

# TABLE OF CONTENTS

# LIST OF TABLES

**TABLE** **PAGE**

# LIST OF FIGURES

**FIGURE** **PAGE**

# LIST OF ABBREVIATIONS AND ACRONYMS

| | |
|---|---|
| PF | Phenol-formaldehyde |
| UF | Urea-formaldehyde |
| MF | Melamine-formaldehyde |
| MUF | Melamine urea-formaldehyde |
| API | Aqueous polymer isocyanate |
| PMDI | Polymeric diphenylmethane diisocyanate |
| PPM | Parts per million |
| WHO | World Health Organization |
| EPA | Environmental Protection Agency |
| IARC | International Agency for Research on Cancer |
| CARB | California Air Resources Board |
| PVA | Polyvinyl alcohol |
| GA | Gum Arabic |
| PVP | Polyvinylpyrrolidone |
| BA | Boric acid |
| AS | Anchote starch |
| VOCs | Volatile organic compounds |
| FTIR | Fourier transforms infrared spectroscopy |
| XRD | X-ray diffraction |
| DSC | Differential scanning Calorimetry |
| TGA | Thermogravimetric Analysis |
| UTM | Universal testing machine |
| SEM | Scanning electron microscope |

| | |
|---|---|
| DS | Degree of substitution |
| RF | Resorcinol formaldehyde |
| EVA | Ethylene vinyl acetate |
| PVAc | Poly vinyl acetate |
| GRAS | Generally recognized as safe |
| USFDA | United States food and drug administration |
| Mpa | Mega pascal |
| ASTM | American society for Testing and materials |
| WT | Wet test |
| WSAD | Water-soaking-and-drying |
| BWT | Boiling water test |
| AA | Acetic anhydride |
| PVP | Polyvinylpyrrolidone |

# ABSTRACT

*Starch is a renewable, biodegradable, and relatively inexpensive natural polymer that originates from different plant sources which attracted much attention in applications of food, papermaking, additives, and adhesives, because of its non-toxicity, renewability, abundance, and good adhesion. It is widely used as adhesives, but the bonding capacity of starch-based adhesive is not strong enough to glues structural products, because, its bond formation is dependent on hydrogen bonding forces, which is the weakest bond of the chemical bonds and it also reacts easily with water molecules to form hydrogen bonds, leading to poor water resistance. Therefore, it is found essential to modify starch to upgrade its adhesive performance for different applications and to replace petroleum derivative adhesives which contain carcinogenic, hazardous, and toxic compounds of formaldehyde.*

*In this study, the starch of anchote (Coccinia abyssinica (Lam.) Cogn.) was extracted using a modified procedure and its functional modification was done by acetalization method. The starch acetates with different degrees of substitution (DS) were prepared by reacting native starch with acetic anhydride using aqueous sodium hydroxide (NaOH) as the catalyst. The degree of substation (DS) increased with increasing temperatures, reaction times, and increasing mixing ratios of acetic anhydride to starch. Increasing the amount of catalyst NaOH up to 30% increases DS and decreases in the interval of 30%-40% due to steric hindrance. The FT-IR analysis confirmed that the introduction of the acetyl group in the acetylated starches through a band at 1739 $cm^{-1}$. X-ray diffraction (XRD) analysis of acetylated starch shown that the crystal structure of native starch was scratched and a new crystalline structure was formed. The scanning electron microscopy (SEM) suggested the starch granules start to rupture and different sizes of cracks are formed on their surfaces when acetalization takes place and eroded surface appearances are observed to make a rough surface than native starch. Differential scanning calorimetry (DSC) confirms that acetalization decreases To, Tp, Tc, and $\Delta H_{gel}$ of starches. The thermal analysis of the native and starch acetate was studied using thermogravimetric (TGA) analysis and differential thermal analysis (DTG), it was found that the thermal stability of acetylated starch depends on the degree of substitution (DS). The thermal stability of acetylated starch with DS-3 is much higher than that of the native starch. This all characterization confirmed the occurrence of structural modification on native starch due to the introduction of the acetyl group on it and its adhesive property measured to be 2.13 Mpa from zero. However, modification of native starch brought significant improvement, but, still can't full filled the minimum criteria of the adhesive which was ≥ 2.32 Mpa. To meet the minimum requirements of adhesive, GA and PVP are incorporated as adhesive enhancers and BA as a Crosslinker. The modified starch adhesive significantly improved to 44.5 Mpa from 2.13 Mpa by incorporating 10% GA, 10% PVP, and 1.5% BA. Its lap shear strength was nearly comparable with commercially available polyvinyl acetate (PVAc) which was 43.13 Mpa. Finally, the occurrence of intermolecular interactions* or *chemical reactions between modified starch, BA, GA, and PVP were proved by FTIR and TGA/DTG analysis. Therefore, this research work concludes that modified anchote starch can be used as a potential raw material for the formulation of adhesives for structural applications.*

***Keywords**: Starch, acetalization, degree of substitution, acetic anhydride, adhesive*

# CHAPTER ONE

# 1. INTRODUCTION

## 1.1. Background of the study

One of the fastest-growing industries in the world is the adhesive industry. Around 20.2 million metric tons of adhesives with a value of 64 billion dollars were produced in 2015[1]. The production of Global adhesive is projected to grow at 4.5% steady annual growth up to 2019 to reach 75.52 billion dollars. It has been used in diversified industries including wood production, paper bonding, automotive, and aerospace. Among these, the structural products industry accounts for 65% of total adhesive applications [1].

Currently, the major adhesives utilized for structural application were synthetic and thermosetting. Depending on their content these adhesives were named phenol-formaldehyde (PF), urea-formaldehyde (UF), melamine-formaldehyde (MF), melamine urea-formaldehyde (MUF), aqueous polymer isocyanate (API), polymeric diphenyl-methane diisocyanate (pMDI), and resorcinol formaldehyde. These synthetic thermosetting adhesives are derived from non-renewable petrochemical raw materials [2, 3], and used for exterior applications because of their superior adhesion bond strength, high water resistance, resistance to environmental degradation, and excellent thermal stability [3-6].

However, with technological advancement, people have begun to realize that non-renewable petrochemical-based adhesives could cause environmental, health, and safety problems by emitting formaldehyde which is a toxic chemical compound. The resulting environmental, health, and safety problems include asthmatic disease, indoor air pollution, damage of the respiratory system, headache, irritation of eyes for a concentration above 0.1 ppm in the air [7]. Depending on its negative impact, formaldehyde has been categorized as a carcinogenic, hazardous, and toxic compound by World Health Organization (WHO) [8], and the Environmental Protection Agency (EPA) since 2008 [3, 5]. In 2004, the International Agency for Research on Cancer (IARC) reclassified formaldehyde from “probable human carcinogen” to “known human carcinogen”. Similarly, the California air resources board (CARB) also formulated regulations with new limits for formaldehyde emissions from composite wood

products. As a result of its non-biodegradable properties, petrochemical-based adhesives could contaminate the environment [7]. Furthermore, as the raw material, petroleum-based chemicals demand were estimated to grow to 50% by 2025, while the oil reserves have been diminishing, The dilemma between the depleting reserve and rising demand may worsen the price on the global market [3, 7]. This diminution of fossil fuel reserve is expected to make the availability of these synthetic petrochemical-based adhesives more expensive in the future [3, 7]. Although there was adverse effect brought by formaldehyde-based adhesives, the market coverage of petroleum-based adhesive bonded wood products is more than 70% of all products [9, 10].

Due to the formaldehyde emission of petrochemical-based adhesives, there was a growing need for alternative adhesives from bio-based sources to solve the problem posed by synthetic petrochemical-based adhesives. Therefore, current researches focus on the development of environmentally friendly, green adhesives from renewable sources, capable of having similar bond strength, excellent water resistance, low cost, less-toxicity, bio-degradable nature that can substitute synthetic and thermosetting petrochemical-based adhesives [3, 7]. Accordingly, the number of patents on bio-based adhesives has boomed by approximately 400 % from 2002 to 2012. Bio-based alternatives gave important promise as they decrease the demand for non-renewable petrochemicals and reduce formaldehyde emissions and other volatile organic compounds [11].

Different kinds of bio-based raw materials have been explored for use in bio-based adhesives. These renewable sources include protein, lignin, tannin, plant oils, and starch. Starch is a renewable, biodegradable, and relatively inexpensive natural polymer that originates from different plant sources which attracted much attention in applications of food, papermaking, additives, and adhesives, because of its non-toxicity, renewability, abundance, and good adhesion [5, 12-14]. It is a promising resource for adhesive production and is composed of two different polysaccharide parts: amylopectin and amylose; both components are composed of a glucose monomer with different shapes and sizes [5, 15]. The amount of amylose to amylopectin ratio differs following the botanical source of the starch and it affects the characteristics of the adhesive [5].

Starch is widely used as adhesives, but the bonding capacity of starch-based adhesive is not strong enough to glues structural products, because, its bond formation is dependent on hydrogen bonding forces, which is the weakest bond of the chemical bonds and it also reacts easily with water molecules to form hydrogen bonds, leading to poor water resistance [5, 12]. These drawbacks seriously restricted the wide utilization of starch adhesives in the structural adhesives field [13].

Therefore, it is found essential to modify starch to upgrade its performance for structural adhesive applications. Grafting copolymerization was one of the techniques for modifying polymers to meet the desired requirements. The grafting of vinyl and acetic anhydride monomers was 0one of the general effective and available methods for the chemical modification of natural polymers [16, 17]. Numerous studies show that starch-based adhesives produced by binding vinyl acetate onto starch using ammonium persulfate as the initiator brought a great improvement of water resistance and bonding strength by converting hydroxyl groups of starch into esters [5, 14, 15]. Another mechanism besides grafting monomer which is used to enhance water resistance and bonding strength of starch-based adhesives is adding materials that have better adhesive characteristics like polyvinyl alcohol (PVA), formaldehyde isocyanate, and tannins [5].

However, there are still substantial challenges for the complete replacement of petroleum-based adhesives with starch-based adhesives, mainly because of their relatively poor water resistance, low bonding strength, and large natural variations due to different growing conditions. There are successful trials for specific starch-based adhesives on how to overcome the drawbacks, but most of them have been tested in laboratory conditions and not in large-scale industrial production. In this respect, fundamental research is still necessary to modify the structure of native starch and study the different factors affecting the formulation of starch-based adhesives from new starch sources.

Therefore, this research mainly focused on using the anchote as a new raw material base for extraction and functional modification of anchote starch for its adhesive property and studying the effect of gum arabic (GA), Polyvinylpyrrolidone (PVP), and boric acid (BA) on its performance improvement.

## 1.2. Statement of the problem

Nowadays, the developments of different manufacturing industries specifically wood works, textile, packaging, shoe, and paper industries are increasing rapidly due to the modernization of the industry, economic development, growing world population, and advancement of living standards. With the increasing of manufacturing industries, the applications of adhesives have risen tremendously to play an important role in manufacturing industries. However, most adhesives used in manufacturing industries are based on non-renewable petrochemical resources, such as urea-formaldehyde, phenol-formaldehyde, and melamine formaldehyde [18]. This heavy dependence on petrochemical raw materials increased the emission of pollutants like formaldehyde and poses human health problems. This indeed required an urgent need for environmentally friendly, non-toxic, biodegradable adhesive originated from renewable sources [12].

Starch is a renewable, biodegradable, versatile, and useful polymer in process industries, not only because is not expensive but also easy to alter its physicochemical properties through modification for the diverse application in industries including adhesive, pharmaceuticals, plastic, cosmetics, detergent, and textile, beverage, building materials, paper, and dye. Starch based-adhesives have been recognized as one of the promising adhesive types in manufacturing industries [19]. However, the performance of starch-based adhesive is usually too weak relative to petroleum-based ones to meet the requirements of manufacturing industries. The poor water resistance, low bonding strength, low mobility, low storage stability, poor weather resistance, and its prone nature to mildew have seriously restricted the wide utilization of starch-based adhesives in manufacturing industries [6].

To improve these drawbacks, numerous studies have been carried out on the functional modifications of native starch. To improve the performance of starch-based adhesive, acid hydrolysis, graft poly-memorization, oxidation, and other starch modification methods have been tried and resulted in better performance improvement concerning bonding strength and water resistance [20]. Nevertheless, compared with petrochemical-based adhesives such as formaldehyde-based resin, the starch-based adhesive is still exhibiting deficiency which impedes their use for many practical applications in manufacturing industries [13].

## 1.3 Objectives of the study

### 1.3.1. General objective

Functional Modification of Anchote Starch: Study on the Effect of Gum Arabic, Polyvinylpyrrolidone, and Boric acid on an acetylated starch Adhesive Performance.

### 1.3.2. Specific objectives

The specific objectives of this research are:

- Extraction and characterization of starch from anchote root.
- Functional modification anchote starch and studying the effect of parameters on modification processes.
- Characterization of acetylated Anchote starch
- Preparation of anchote starch-based adhesive and studying the effect of modified starch, gum arabic (BA), boric acid (BA), and Polyvinylpyrrolidone (PVP) on its performance.
- Characterization of prepared anchote starch-based adhesive

## 1.4. Scope of the study

The scope of this thesis work mainly focus on:

- Extracting and characterizing anchote starch
- Modification of anchote starch and studying of processing parameters, reaction temperature, reaction time, mixing ratio, and catalyst loading.
- Characterizing modified and native anchote starch by using instrumental techniques such as Scanning electron microscope (SEM), Fourier transforms infrared spectroscopy (FTIR), x-ray diffraction (XRD), Differential scanning calorimetry (DSC), and Thermogravimetric Analysis (TGA).
- Formulating anchote starch-based adhesive and studying the effect of modified starch, gum arabic (GA), and Polyvinylpyrrolidone (PVP) on its performance.
- Characterizing the formulated anchote starch adhesive by instrumental techniques, Fourier transforms infrared spectroscopy (FTIR), and Thermogravimetric Analysis (TGA).

## 1.5. Significance of the study

Preparation of modified anchote starch which was used as a raw material for better-performing starch-based adhesive in terms of bonding strength and water resistance to replacing petrochemical-based adhesives was a significant contribution to this thesis. Using a cheap, locally available, environmentally friendly, and bio-degradable raw material reduces the dependence on petroleum-based raw materials for adhesive production. In terms of environmental and health aspects, starch-based adhesive reduces the emission of volatile organic compounds (VOCs). This will reduce the cause of indoor air pollution that may pose the danger of cancer and respiratory problems like asthma. It also minimizes contamination of underground water and soil by reducing non-degradable matters by substituting those using biodegradable raw materials. Economically it has big significance on import substitution of petroleum derivatives as a raw material. Therefore, this research has a higher contribution to the economy, environment, and public health.

# CHAPTER TWO

# 2. LITERATURE REVIEW

## 2.1. Anchote (Coccinia abyssinica)

Anchote is the vernacular name for (*Coccinia abyssinica* (Lam.) Cogn.); spelled as ancoote in Afan Oromo, belongs to the genus *Coccinia [21]*, order *Cucurbitales* [21-26], and family *Cucurbitaceae* [21, 23, 24, 27, 28], which is indigenous root tuberous crop for Ethiopia[23, 29-31]. It is also an annual trailing vine nutraceutical plant that has shoots with simple tendrils, and leaves. Leaves are palmate simple with five lobes, while the shape varies from the heart to pentagon form, fig.2.1. Fruits are red yellow at maturity and have an oval to cylindrical shape containing an average of 153 seeds [32]. Anchote has spherical to cone-shaped tubers which may vary with age, soil physical conditions, and anchote type.

Figure 2. 1 Anchote plant and roots[33]

It is cultivated for human consumption throughout the south and southwestern parts of Ethiopia for centuries [32]. Contrasting to many other root crops, anchote can grow with minimum inputs and its yield practically is good under unfavorable situations such as low soil fertility, acidic soils, drought, and under intercropping with cereals [34]. It grows principally for its tuberous root, but its leaf and fruits are edible as a cooked green vegetable, which makes it a versatile crop [35]. Based on tuber colors, two types of anchote are known by local names as 'Diimaa'

and ‘adii’ in Oromiya especially in Wollega, meaning red and white, respectively as shown in fig.2.2 [33].

Figure 2. 2 Red and white anchote roots[33]

It is also known by different vernacular names in different parts of Ethiopia, such as ‘*ushushe’* in Wolayita, ‘*shushe’* in Dawuro and ‘*ajjo’* in Kaffa, and ‘*wouchich*’ in Tigray [24, 26, 36]. In Ethiopia, the cultivation of anchote as a root crop is sporadic but well-known in the Western and Southwestern parts of Wollega, Kellam Wollega, Mattu, Jimma, Iluababor, Kaffa, Sidamo [22, 34]. Also [37], reported that anchote was found in the Amara region specifically in Gonder, Gojam, and Bale area in Oromiya, however, its level of cultivation and utilization was not reported.

Anchote exists both as a cultivated and wild plant with a wide distribution in Ethiopia especially south and southwestern parts [31]. The crop is adapted to grow at an altitude range from 1,300 to 2,800 meters above sea level with an estimated annual rainfall range of 762- 1,016 mm per year [30]. It prefers soil with a pH of 4.5 to 7.5, and a temperature with a minimum and maximum of 12 $^{0}$C and 28 $^{0}$C respectively [38, 39]. Farming methods are propagation, husbandry, harvesting, and postharvest handling [32]. Farmers usually plant Anchote on a piece of land not more than 400-600 square meters in the backyard mainly for home consumption in the western Oromia zone. The land coved by tuber crops in this area is nearly 300 hectares, yielding on average 150-180 quintals per hectare [25, 40].

Anchote reaches its maturation stage within 4 to 5 months from planting depending on the environmental condition and type of tubers [38, 41].

## 2.2. Uses and composition of Anchote *(Coccinia abyssinica)*

### 2.2.1. Uses of Anchote (*Coccinia abyssinica*)

The most important part of Anchote is its tuberous root. It has potentials for human nutrition, animal feed, medicinal application, and starch production. It plays great importance in food security, income generation, cultural and social purposes [42]. Anchote is strongly associated with the cultural value of the Oromo people, as a prestige dish prepared for ceremonies and festivals in Oromo's culture[32, 43]. Similarly, the same authors reported that the traditionally prepared anchote has active component "Saponin" which is used as a traditional medicine to treat diseases like gonorrhea, tuberculosis, tumor cancer, diabetes, asthma, and cholesterol-lowering. Also, the soup and juice made from red Anchote are used as a feed supplement to persons with fractured bones and displaced joints, as it contains high calcium content and proteins than other root and tuber crops. Traditionally, it is believed that red Anchote's active ingredient helps lactating mothers to become healthier and stronger [32].

### 2.2.2. Composition of Anchote *(Coccinia abyssinica)*

The nutritional composition of anchote tubers based on the wet weight basis of the sample is shown in the table below.

Table 2. 1 Proximate composition of anchote (w/w % in dry basis) [23]

| Sample | Total starch(% ) | Crude Protein(% ) | fat(% ) | Moisture content(% ) | Ash (% ) |
|---|---|---|---|---|---|
| Anchote starch | 78.71 | 0.34 | 0.2 | 9.06 | 0.3 |

## 2.3. Extraction and Physico-chemical characterization of anchote starch

Abera, Woldeyes et al reported the extraction of the anchote tuber starch using a modified procedure. According to their report anchote starch has unique structural and functional properties (granule size, shape, morphology, thermal stability, and crystallinity) that make it different from other starches like corn and potato. A proper understanding of such unique property is very crucial to develop optimum extraction and to modify starch for different applications. These different properties of anchote starch are reported by the different authors.

The morphological structures of anchote starch granules were evaluated using SEM and the size of granules was varied from 1.31 to 18.09 μm and it was too much smaller than that of wheat and potato starches. The x-ray diffraction analysis of anchote starch showed a B-type starch. It has also a greater gelatinization temperature of 66.58 °C, which indicates that the more crystallinity or high amylopectin component in anchote starch. The thermal stability of anchote starch relative to potato and wheat. According to this analysis, anchote starch is more thermal stable than potato and wheat starches. Therefore, the Anchote starch paste had better resistance for heating and shearing. The thermal stability, very small granule size of starch, and shear resistance make anchote starch a potential candidate for thermoplastic starch products including adhesives, plastics, and others [23].

## 2.4. Chemistry of Starch

Starch is the most abundantly available polysaccharide biomaterial next to cellulose in seed crops and root tubers. It serves as a kind of energy storage for plants [45, 46]. It constitutes two types of D-glucose which are amylopectin (highly branched or branched nearly every 20 glucose units) and Amylose (un-branched or branch approximately every two hundred glucose units). Amylose is a linear molecule of anhydrous glucose units that are linked mainly by α-(1–4)-D-glycoside bonds as shown in fig.2.4. Amylopectin is a Linear α -1, 4 chain with an α-(1,6) D-glycosides bonds as shown below in fig.2.4 with the average molecular weight (M) of $10^6$ Da and$10^8$ Da respectively [47-49].Starch is a simple carbohydrate comprising of a huge number of glucose units which is extremely common in the human diet and is confined in large amounts in staple food such as wheat, potato, maize rice, and cassava. It is one of the most versatile biomaterials which received greater attention recently for different applications like food, textile, cosmetics, plastics, adhesives, paper, and pharmaceutical industries [50].

This is due to its biocompatibility, biodegradability, non-toxicity, abundance, low cost, high caloric value, inherent excellence physicochemical properties, and the ease of its modification to other derivatives[45].

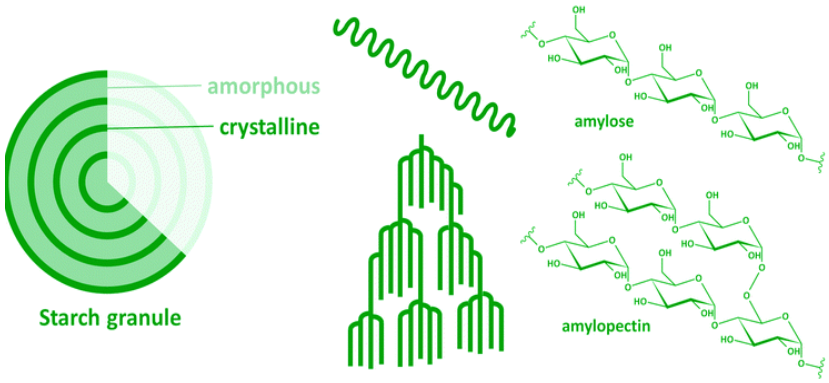


Figure 2. 3 Starch granule structure [51]

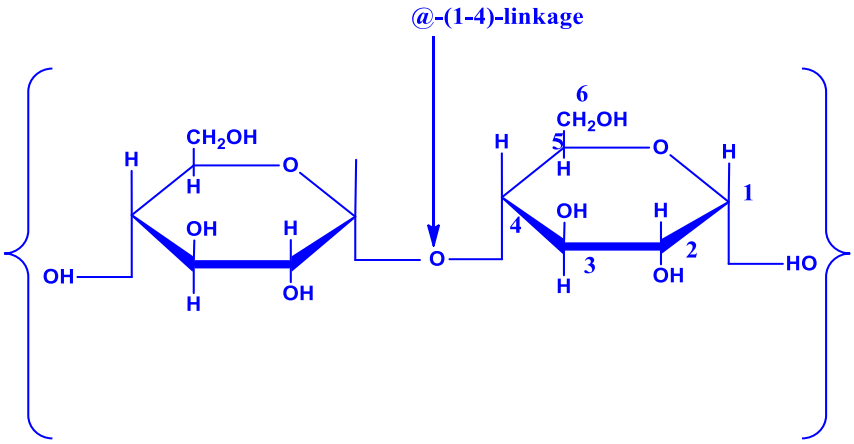


(A)

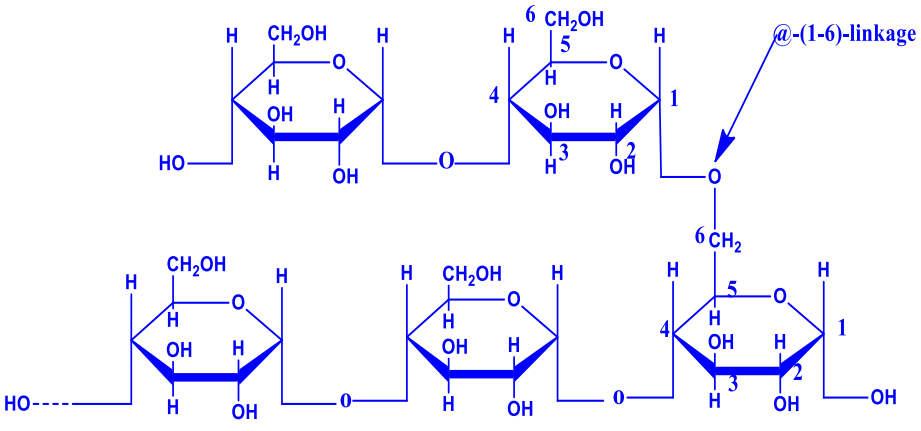


(B)

Figure 2. 4 (A) Amylose, and (B) Amylopectin [51]

## 2.5. Starch Application for adhesives

Starch has various applications in the productions of food and other non-food industries [52]. As the most abundant natural polysaccharide macromolecules, starch has a potential application in the starch-based adhesive. Also, it has been extensively investigated and widely used in the adhesives industry due to its relatively great adhesion performance and zero formaldehyde emission to the environment. But its bonding strength is insufficient for bonding structural products [53]. It is an attractive green material to replace petrochemical-based ingredients in adhesives. Since the demand for adhesives is increasing in recent years applications of substitute raw materials will be very important.

The industry of adhesive is highly reliant on petroleum-based resources because of their high performance and low cost. However, adhesives from petroleum-based ingredients can cause severe risks to the health of human beings and polluting indoor air quality by releasing cancer-causing compounds. Therefore, there is an increasing demand to substitute the petrochemical-based ingredients in the formulation of the structural adhesive with green renewable raw materials. Starch is one of the most abundant green biopolymers and is used as energy storage in numerous plants including cereals, tubers, roots, fruits, and seeds [53, 54]. But, its physical and chemical properties in its native form do not make it preferable for structural adhesive formulation. It has poor shear and thermal stability and a high degree of retrogradation. Additionally, the native form of starch can simply undertake syneresis beyond the gelling tendency of the pastes [52]. Therefore, the physical and chemical properties of starch are very important to be used in numerous industries like adhesive, food, paper, and textile. It can be improved by implementing various techniques of modification.

### 2.5.1. Modification of Starch

To enhance specific functional properties, starches are often modified by physical, chemical, and enzymatic processes. The physical modification method of starch is done by moisture, heat, shear, or radiation and this mechanism of modification has been gaining attention because of the nonexistence of chemical reagents in the modified starch. Chemical modification is a widely applied and very common method to alter the properties of starch for different applications. Chemically modified starches have a range of physical and chemical properties which make them available for different uses because they show excellent physicochemical properties that are improved from those of their native starches.

**2.5.1.1. Modification of starch by Acetilazation**

Starch Acetylation is a well-known chemical modification technique in which, the hydroxyl (OH) functional groups of the glucose molecule are substituted by the acetyl group and modify the molecular structure of the starch. These modified starches are produced by using acetic anhydride and an alkaline catalyst such as sodium hydroxide (NaOH). Acetylated starches performed different functions depending upon the degree of substitution (DS). Starches with low DS of (0.01- 0.2) may act as adhesion, thickening, texturizing, film-forming, stabilizing, and binding agents and also find numerous applications in the food industry. Modified starch with an intermediate DS of (0.2-1.5) and a high DS of (1.5-3.0) have been described for their high solubility in polar solvents like acetone and chloroform and thus, can be used as a thermoplastic material. Starch acetylation is performed to bring changes in the physical, functional, and chemical properties of starches and has been used by many researchers. Different factors play a vital role in the inducement of changes caused by acetylation. These factors include the source, ratio of amylose and amylopectin, the molecular structure of starch, and the degree of substitution. The reaction efficiency and the number of acetyl groups induced in the starch molecule during the process of acetylation depend upon the reaction time, presence of the catalyst, botanical origin, reagent concentration, and structural characteristics of starch granules. Reaction of starch by acetic anhydride shown in fig.2.5 below

$$St\text{-}OH + OH^{(-)+} (CH3CO)_2O \text{-----} St\text{-}OCOCH_3 + CH_3COO^{(-)} + H_2O \text{ …..(2.1)}$$

St-OH = Starch

$(CH_3CO)_2O$ = Acetic anhydride

$St\text{-}OCOCH_3$ = Starch acetate

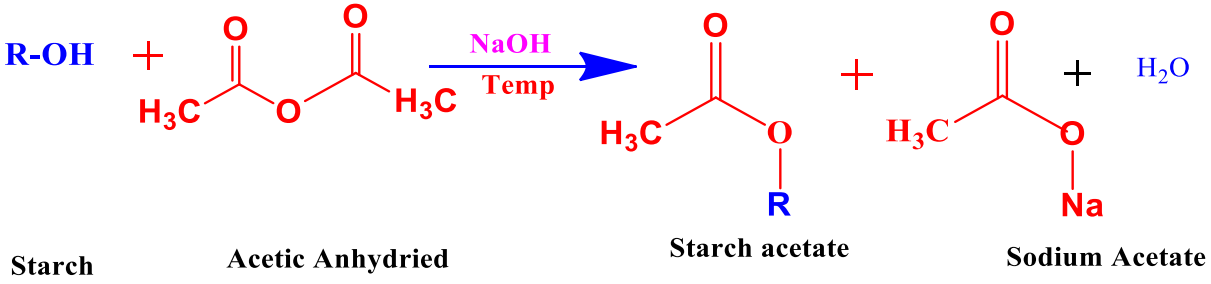


Figure 2. 5 Reaction of starch with acetic anhydride

Table 2. 2 Related works on starch acetylation

| Product | Starch in dry base | Reagent | Solvent (ml) | Catalyst | Reaction condition | Wash solvent | Degree of substitution (DS) | Reference |
|---|---|---|---|---|---|---|---|---|
| Starch acetate | 30 g | Acetic anhydride 76 g | Acetic anhydride | 10.2 g 50% aqueous NaOH | 123 °C, 4h | Water | 2.59 | [56] |
| Starch acetate | 10 g | Acetic anhydride, 30 g | 10 mL Acetic Acid | 0.38 mL $H_2SO_4$ | 70 °C, 3h | Water | 2.67 | [56] |
| Starch acetate | 30 g | Acetic anhydride 54 ml | Acetic acid 55 ml | 0.38 mL of the methyl sulfonic acid | 90 °C, 0.5 h | Ethanol | 1.9 | [57] |
| Starch acetate | 30 g | Acetic anhydride 54 ml | Acetic acid 55 ml | 0.38 mL of the methyl sulfonic acid | 90 °C, 1.5h | Ethanol | 2.4 | [57] |

| | | | | | | | | |
|---|---|---|---|---|---|---|---|---|
| Starch acetate | 30 g | Acetic anhydride 54 ml | Acetic acid 55 ml | 0.38 mL of the methyl sulfonic acid | 90 °C, 2h | Ethanol | 2.9 | [57] |
| Starch acetate | 30 mmole | Acetic anhydride 90 mmole | 90 mmole | Iodine | 100 $^{0}$C,2h | Ethanol | 2.93 | [58] |
| Starch acetate | 40 g | Acetic anhydride 76 ml | Acetic anhydride | 10% NaOH | 123 $^{0}$C,4h | Water | 1.36 | [59] |
| Starch acetate | 15 g | Acetic anhydride 130 mL | | 3 mL of 50% p/v NaOH | 123 $^{0}$C,3h | Water | 1.6 | [60] |

.

Generally, starch acetate with different degree of substitution were observed at different reagents and reaction conditions for different applications like food additives, coatings, cigarette filters, biodegradable packaging materials, tablet binders, and other pharmaceutical applications. From my knowledge there no study was done on adhesive property of starch acetate with high degree of substitution Therefore, study on modification of anchote starch acetate with higher degree of substitution for its adhesive application was done by incorporating PVP and GA as Crosslinker and BA as Crosslinker.

### 2.5.2. Modification of starch by grafting

Grafting is an essential method for modifying the Physico-chemical properties of polymers. Grafting polymerization of man-made polymers onto a starch backbone is one of the effective ways of enhancing the bonding properties of starch-based adhesive [61, 62]. There are numerous researches on the synthesis, characterization, and properties of starch graft copolymers, and some of them are tabulated as follows in Table 2.4

Table 2. 3 Related works on grafting of starch.

| Graft on | Grafted by | Bond strength improvement | | Improvement of water resistivity | Reference |
|---|---|---|---|---|---|
| | | Dry state | Wet state | | |
| Starch | Vinyl acetate | 59.4% | 321% | 61.1%. | [62] |
| Starch | Vinyl acetate and hexyl acrylate | 11.23 MPa | 5.63 Mpa | Improved | [12] |
| Starch | Itaconic acid (IA) | 43.6% | 93.2% | Improved | [63] |
| Starch | Silane coupling agent and olefin | 7.88 MPa | 4.09 Mpa | Improved | [52] |
| Starch | Dodecyl succinic anhydride (DDSA) | 2..6 MPa | 72.4% | 72.4% | [20] |

## 2.6. Adhesives

Adhesion is the tendency of dissimilar substrates to attach by the attraction force between two substrates as a result of intermolecular forces established between adhesive and substrates [64]. A substrate held to another substrate by an adhesive is called an adherend. The attraction force is formed by the interactions of atoms, ions, and molecules that exist within and at the surfaces of both adhesive and adherend. Mechanical bonding of the surface of adhered are held together by an adhesive which has penetrated through a porous surface while it is liquid, then attached itself during curing [65]. The bond-forming process between dissimilar adhesive and substrate is called adhesion as well as the bond-forming process that takes place between similar molecules of adhesives to stick together is called cohesion [66]. Adhesion and cohesion processes shown in fig.2.6 below.

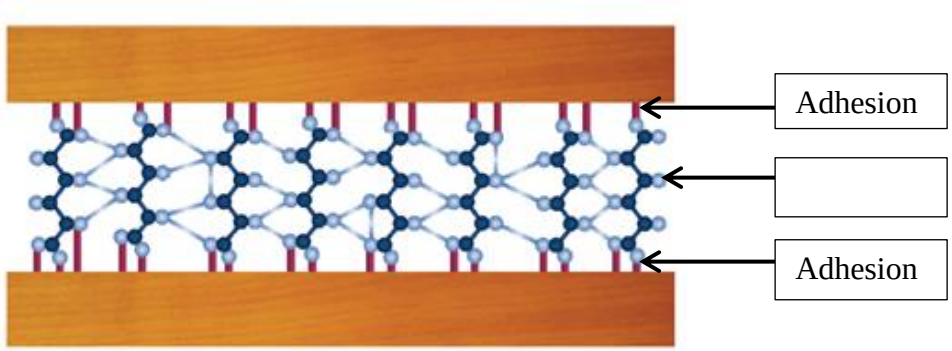


Figure 2. 6 Adhesion and cohesion mechanism adapted from [67]

### 2.6.1. Adhesion Mechanisms

Basic knowledge of adhesion mechanisms is very important to develop high-performing adhesives in engineered wood products [68]. Numerous theories of adhesion mechanisms have been proposed in the last few decades to describe the adhesion mechanism between substrate surface and adhesive. Among them, electronic, boundary layers and interfaces, mechanical interlocking, adsorption, diffusion, and chemical bonding are considered to be the leading theories [69, 70].

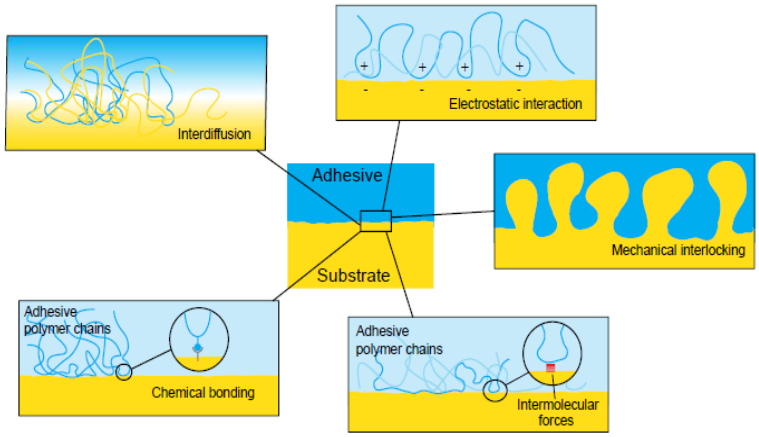


Figure 2. 7 Adhesion mechanism adapted from [71]

The mechanical interlocking theory is the first theory on adhesion mechanism. According to mechanical interlocking theory, adhesive spread and penetrate the fibers cells through the capillary path, cavities, and surface of substrates to displace trapped air, followed by gluing of the substrate to provides strength by interlocking during curing as shown on fig.2.7 above [72]. Wetting of the substrate surface is critical in mechanical interlocking theory, where adhesive requires diffusion into the wood. Therefore, the rheological property of the adhesive also plays an essential part in mechanical interlocking [73]. Effective mechanical interlocking happens when the penetration of adhesive beyond the surface debris and hurt fibers into wood up to six cells deep [15].

Deeper diffusion into the microstructure of the wood sample increases the area of contact between adhesive and substrate for more effective mechanical interlocking. The toughest structural bonds to wood substrates are supposed to be developed not only when an adhesive goes deep in cell cavities, but also when it penetrates cell walls to make molecular-level contact with the structure of the wood sample. If an adhesive enters deep enough into a wooden substrate and becomes tough enough upon curing, the bond strength can be expected to exceed the strength of the wood [65].

The adsorption theory suggests that the substrates are to be adhered to due to intermolecular and interatomic forces that arise between the atoms and molecules in the adhesive and substrate upon their bonding [72]. According to adsorption theory, primary interactions such as covalent, ionic, and metallic bonds; and donor-acceptor interactions; secondary interactions such as van der Waals forces and hydrogen bonds are the primary contributing forces in adhesion [74].

Adsorption theory also recommends the significance of surface roughness and wetting of the surface as crucial factors in adhesion mechanisms [72].

Interdiffusion theory defines adhesion as a process arising due to the Interdiffusion of macromolecules from two polymeric materials at the adhesion interface. Therefore, both adhesive and the adherend are supposed to be polymeric materials that are mutually miscible and compatible [72]. The nature of the polymeric materials such as chain length and molecular movements of the materials play a crucial role in Interdiffusion theory [74]. Electrostatic attraction theory is a type of adhesion that the adhesion mechanism depends on the linkage of adhered and adhesive at the interface by mutual sharing of electrons. As a result of the difference in electronic charge of the adhesive and adherend at the boundary layer, the electron transmission between two materials will be activated, creating a double layer of electrical charge that improves adhesion between two surfaces [75]. Therefore, based upon this theory, both surfaces should have been charged positively and negatively to activate the adhesion mechanism [72]. Chemical bonding theory suggests that a bond formed between adherend and adhesive at the interface is the main factor in the adhesion mechanism of two materials. In this theory Dipole-dipole Intermolecular force interactions and primary chemical bonds are considered to be the primary means of adhesion mechanism[72]. Well-matched functional groups existing in adherend and the adhesive surface will create interactions; thus adhesion mechanism will rely on the type and number of bonds formed in the adhesion interface [76].

### 2.6.2. Adhesive Failure

Generally, the strength of adhesion is measured by applying a tensile force perpendicular to the adhesion surface, and the maximum tensile force required to break the bond of the interface will be recorded. The possibilities of bond failure at the adhesion interface are shown in the schematic representation below.

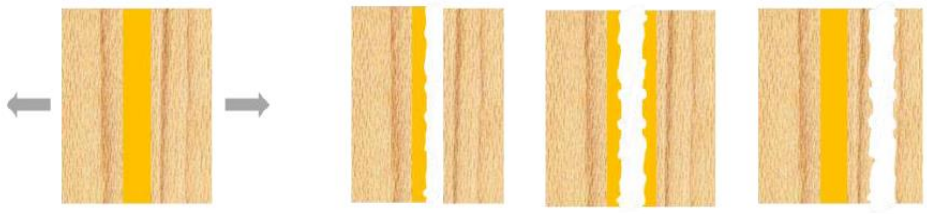

(A) (B) (C)

Figure 2. 8 (A) Adhesive (B) Cohesive (C) Cohesive failure [71]

In fig. 2.8-A, the bond failure occurred between the adhesive, and one of the adherend surfaces, and this kind of scenario is called adhesive failure. In fig 2.8-B, the bond failure occurred between adhesive molecules while both adherend surfaces remain covered with an adhesive layer and this failure is because of cohesive failure in the adhesive. Similarly, in fig 2.8-C, the bond failure that occurred between adherend surfaces while adhesive molecules remain bonded within the adhesive layer is called cohesive failure in adherend. In this case, adhesive bonds have excellent strength that exceeds the strength of adherend bond strength [77]

## 2.7. Adhesive properties of PVP and Gum Arabic (GA)

### 2.7.1 Adhesive properties of PVP

Polyvinylpyrrolidone (PVP), also called povidone, was first developed by Walter Reppe of BASF in the late 1930s. PVP is a special and uncommon material as it can be solvable in both water and various organic solvents, such as alcohols, amines, acids, chlorinated hydrocarbons, amides, and lactams. PVP has the linear formula $[C_6H_9NO]$ n with a molecular weight of 40,000 and a melting point of 172 $^0$C. It has a viscosity of 26 cps and PVP k-30 has hydrophilic as well as hydrophobic functional groups, which can interact with different solvents. PVP is a synthetic and biodegradable polymer [78, 79]. These unique properties made it suitable for numerous applications such as pharmaceuticals, cosmetics, beverages, adhesives, detergents, paints, electronics, and biological engineering materials. , Due to its specific advantages, like good adhesion property, excellent physiological compatibility, low chemical toxicity, high hydrophobicity, good complication property, firm-forming ability, reasonable solubility it has a wide application [80].

Adhesion is a crucial surface characterization for PVP and humidity is an essential factor to adjust the adhesion property of PVP. Researchers investigated that the effect of relative humidity (RH) on the intrinsic adhesion forces of PVP toward both hydrophobic and hydrophilic pharmaceutical materials and they found that the effect of RH on adhesion force was more significant for the PVP/hydrophilic material than the PVP/hydrophobic material [79]. Report of [78] shows that the shear strength of the adhesive made from dissolving 8 grams of polyvinyl pyrrolidone (PVP) in 50 ml of ethanol alcohol with purity 99.9% was best at a temperature of 225 $^0$C and curing time of 10 minutes. Fig.2.9 shows the structural representation of PVP.

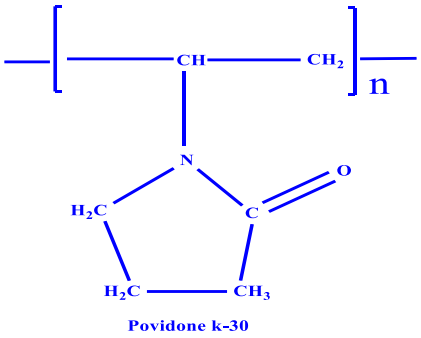


Figure 2. 9 Polyvinylpyrrolidone structure [80]

### 2.7.2. Adhesive property of Gum Arabica (GA)

From different polysaccharides, gum Arabic (GA) is a biocompatible, and biodegradable polysaccharide derived from an exudate of *Acacia Senegal and Acacia Seyal* trees. Gum Arabic is a neutral or somewhat acidic salt of polysaccharide containing calcium, potassium, and magnesium cations. GA is used in wide application areas such as adhesive, ceramics, textiles, cosmetics, pharmaceuticals, and food processing. It is used as a thickener, emulsifier, and stabilizing agent. It also has been given a generally recognized as safe (GRAS) status by the united states food and drug administration (USFDA) [81]. Fig.2.10 shows the structure of GA.

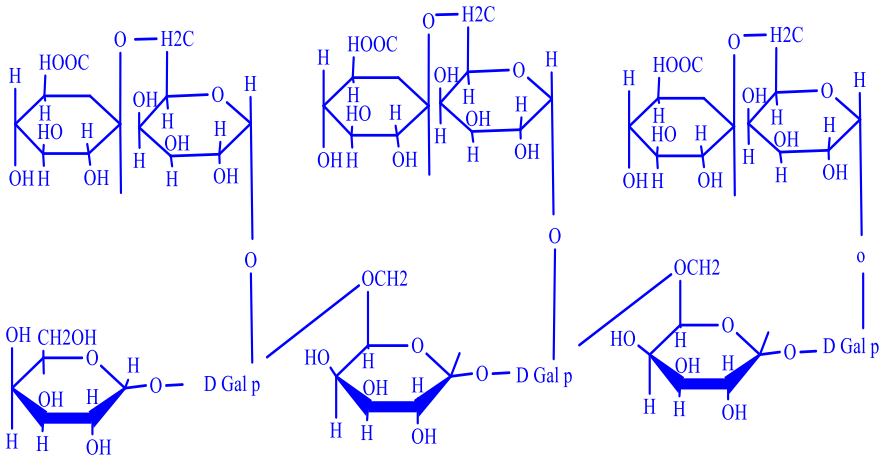


Figure 2. 10 Structure of Gum Arabic

GA shows good adhesive characteristics for soft substrates such as paper, but the adhesive characteristics of this polysaccharide are highly affected by its hydrophilic nature. Environmentally friendly wood adhesives are prepared by dispersing other gum types like guar gum, xanthan, locust bean gum, and tamarind gum. In previously done researches, the gum-

based adhesives were prepared by adding the gum in deionized water and heating at 60 $^{0}$C for 6 hr. in the oil bath. The quality of the adhesives was tested by applying the adhesive on glass surfaces. It was observed that the locust bean gum and guar gum form uniform and non-smooth surfaces when applied. The clear and smooth film was produced by xanthan gum mixing. The lap shear strength of all types of gums applied on the wood substrate was less than 16 MPa. Hence, it was concluded that the gums were evaluated to be used as wood adhesives [81].

## 2.8. Crosslinker effect on starch-based Adhesive

Cross-linking is the common method to increase the performance of starch for numerous applications. Starch and starch-based products have been cross-linked with cross-linking agents, such as phosphorus oxychloride, sodium trimetaphosphate, sodium tripolyphosphate, and epichlorohydrin. The cross-linking helps to improve the mechanical properties and water stability of starch products. In addition to cross-linking, the blending of starch with synthetic polymer has also been considered to improve the performance of starch-based products. PVA is well suited to be blended with natural polymer since it is highly polar and readily soluble in water. Boric acid is a commonly used cross-linker for starch and PVA for various applications. Most of the time, PVA is mixed with starch to reduce the overall cost of the blend. [82-85].

In this study, a starch-GA-PVP mixture is prepared in a water solution coupled with boric acid as a cross-linking material to observe the effect on the physical, mechanical, and thermal properties of blended adhesives. The crosslinking of starch and GA with boric acid takes place in the mixture as shown in the fig.2.11 below

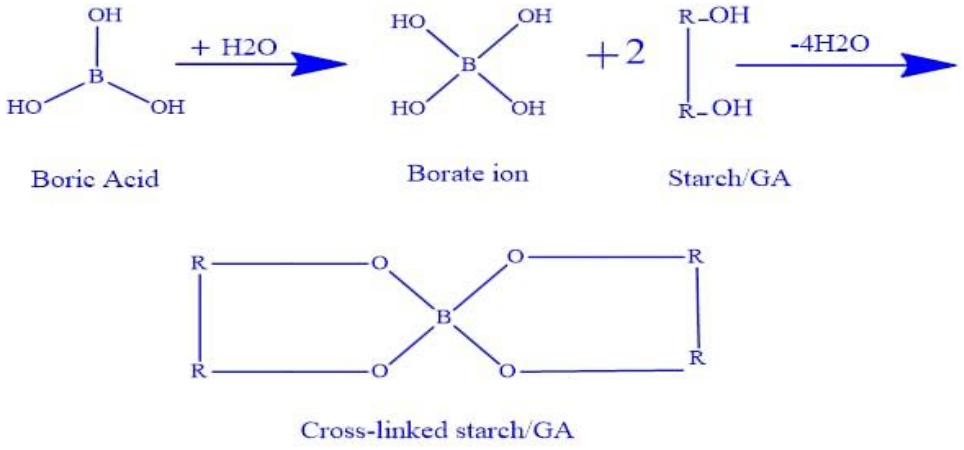


Figure 2. 11 Cross-linking mechanism of boric acid [85]

## 2.9. Bonding strength and water resistance evaluation of adhesive

Shear strength is used to evaluate the bonding strength of adhesives and the mechanical properties of composites. There are several standards to measure the shear strength of the adhesive-bonded composites such as the ASTM standard test method for strength properties of adhesive bonds in shear by compression loading (D 905, D 4262, and D 2559), the European Standard EN 205, and the China National Standard (GB/T 17657-2013). As described in these standards. In the shear test, one end of each sample is glued by adhesives and the other end is inserted into the clamps of the tensile machine and moved up at a certain speed until the bonded sample are detached. To interpret the recorded bonding strength of adhesives, it is crucial to know where the failure occurred in the tensile tests.

Water resistance of wood adhesive bonding plays a crucial role in the mechanical properties of wood adhesive in its application in the wood composites industry. The bonded wood with high water resistance is preferable for exterior applications, while the bonded wood with mild water resistance is appropriate for interior applications. Water resistance can be determined based on ASTM Standard Methods D1183-96 [86], D1151-00 [87, 88]. As explained in these standard methods, the bonded wood composite is tested for different conditions as the wet test (WT), water-soaking-and-drying (WSAD) test, and boiling water test (BWT). For the WT, the bonded specimen is soaked in water at 23 ◦C for 48 h, then evaluated immediately for wet shear strength [2].

# CHAPTER THREE

# 3. MATERIALS AND METHODS

## 3.1. Materials

### 3.1.1. Chemicals and apparatuses

Freshly harvested anchote tuber collected from Guto Gida district of Wollega, Acetic anhydride $(CH_3CO)_2O$ from Hindustan Speciality chemicals, India Polyvinyl-pyrrolidone(PVP) K-30 from Otto Chemie Pvt.Ltd, India, Sodium metabisulphite ($Na_2S_2O_5$) from Qingdao Tianya Chemical Co., Ltd, China, Hydrochloric acid (HCl) from Indiamart Pvt.Ltd, India, Gum Arabic (GA) ($C_{15}H_{20}NNaO_4$) from Shaanxi Bloom Tech Co., Ltd, Sodium hydroxide (NaOH) from Indiamart Pvt.Ltd, India, Petroleum ether ($C_6H_{14}$**)** form Indiamart Pvt.Ltd, India, Boric acid ($H_3BO_3$) from Indiamart Pvt.Ltd, India, and distilled water from Adama Science and Technology university Chemical Engineering Laboratory. The materials used for this thesis work during the laboratory activities were Soxhlet extractor, ball mill, mechanical blender, mixer, sieve with 250µm, knife, beakers, flasks, measuring cylinder, spatula, petri dish, goggles, gloves, pipette, dropper, ice bath, water bath, filter paper, analytical balance, vacuum desiccator, pH meter, flasks, oven drier, magnetic strier, and universal indicator. All chemicals were laboratory grade and used without further modification. Wood pieces were purchased from locally available wood workshops in Adama, Ethiopia to be utilized in lap shear tests.

## 3.2. Methods

### 3.2.1. Sample collection and preparation

Freshly harvested anchote samples were collected from the Guto Gida district of Wollega, Ethiopia, and transported to the chemical engineering laboratory of Adama Science and Technology University

### 3.2.2. Extraction of starch from Anchote

The starch of Anchote tuber was isolated using a modified procedure followed by[89]. The raw Anchote tuber was washed to remove debris from the surface and peeled. The peeled tuber was cut into approximately 1 cm cubes. The size was further reduced using a mechanical shredder for 5 min to get the crushed anchote tuber with a uniform size. A 10 % (w/v) crushed tuber and tap water suspension was prepared. The suspension was filtered with a 250 μm sieve and the filtrate was kept for 12 h. The supernatant is decanted and the sediment was washed until it became pure white. The sediment was dried at 40 °C for 48 h in an oven. The starch powder was made from dried sediment using a ball mill.

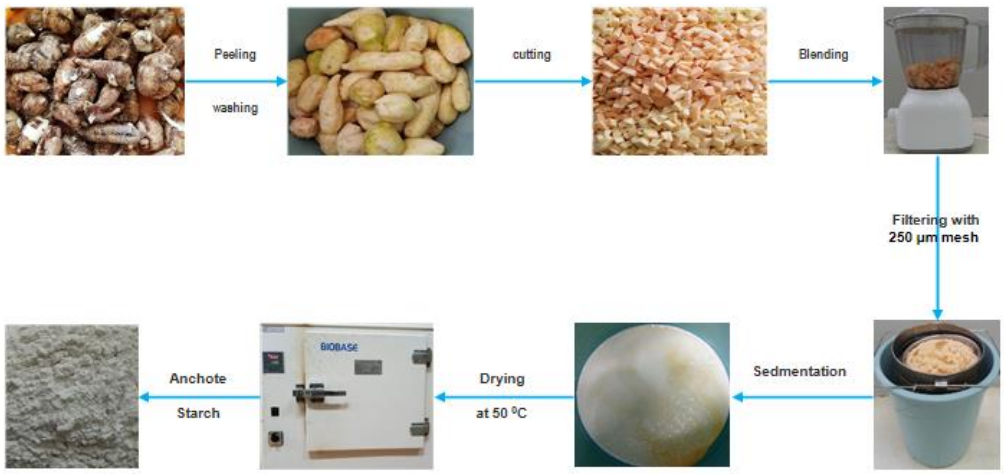


Figure 3. 1 Experimental procedure to extract starch from anchote

### 3.2.3. Modification of Anchote Starch

Anchote Starch acetylation was conducted by a modification procedure of [90]. Before acetylating, anchote starch was dried in an oven for 24 hr. at 50 °C. Dried starch (15 g) was mixed with acetic anhydride at weight ratios of 1: 0.5, 1:1, 1:2, and 1:3 in a beaker. After stirring for 5 min, 50% aqueous NaOH solution was added as a reaction catalyst. The temperatures of 80 °C, 85 °C, 90 °C, and 100 °C were used for the reaction for the designated times of 60, 120, 180, and 240 min. The NaOH was added at different mass ratios of 0.1, 0.2, 0.3, and 0.4 g/g, of starch. To study the effects of each variable (mixing ratio of starch and acetic anhydride, temperature, reaction time, and catalyst loading) on the degree of substitution one variable at a time method was applied. Excess distilled cold water was added to the reactor to terminate the

reaction and to wash the reaction products after the reaction time is reached. The acetylated starch was dried at 50°C. Finally, the dried products were ground before testing.

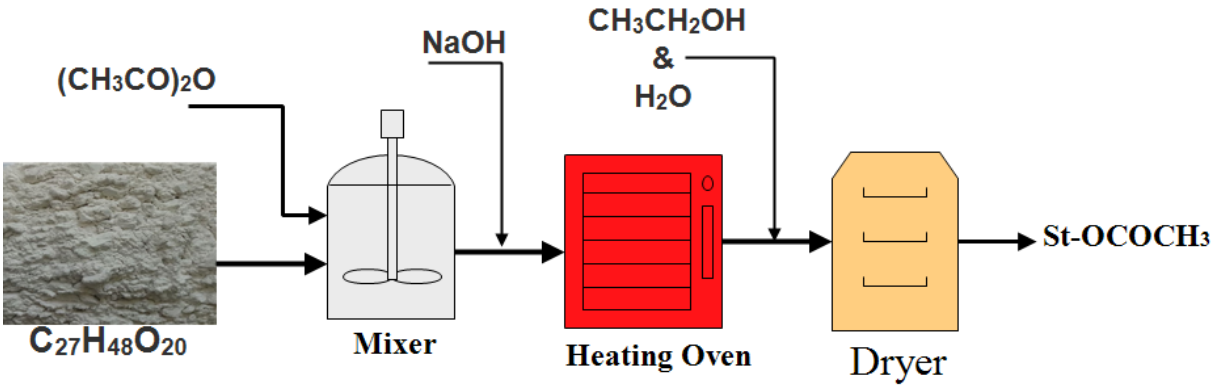


Figure 3. 2 Experimental procedure for modification of starch

### 3.2.4. Determination of degree of substitution

The DS of starch acetate was determined by back titration using the method of [91]. An amount of 0.5 g of acetylated starch was placed in a 250 mL vessel with distilled water (50 mL) and the pH was adjusted to 7 with 0.02 N HCl. Then 25 mL of 0.5 N NaOH was added and heated on a hot plate with vigorous stirring until a clear solution was obtained. The excess NaOH was titrated back to pH =7 with HCl 0.02 N. The DS was calculated as in [55]:

$$\text{Degree of substitution} = \frac{162*(\text{N NaOH}*\text{V NaOH}-\text{N HCl}*\text{V HCl})}{1000*W-42*(\text{N NaOH}*\text{V NaOH}-\text{N HCl}*\text{V HCl})}$$

where $N_{NaOH}$ was the normality of NaOH, $V_{NaOH}$ was the volume of NaOH, $N_{HCl}$ was the normality of HCl used to back titrate, $V_{HCl}$ was the volume of HCl used to back titrate, and W was the sample weight (g).

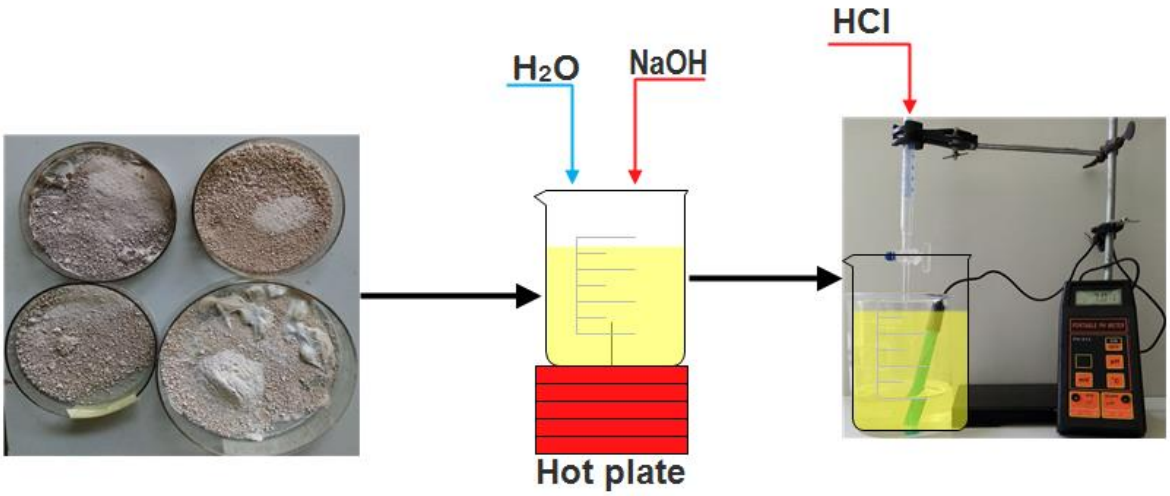


Figure 3. 3 Experimental procedure to determine DS

Table 3. 1 Effect of temperature on Degree of substitution

| Temperature ( $^0$C ) | Mixing ratio(w/w) | Reaction time(m) | Catalyst loading (w/w) | Degree of substitution (DS) |
|---|---|---|---|---|
| 80 | 1:2 | 180 | 0.3 | |
| 85 | 1:2 | 180 | 0.3 | |
| 90 | 1:2 | 180 | 0.3 | |
| 100 | 1:2 | 180 | 0.3 | |

Table 3. 2 Effect of reactant/ raw material mixing on Degree of substitution

| Temperature ( $^0$C ) | Mixing ratio(w/w) | Reaction time(m) | Catalyst loading (w/w) | Degree of substitution (DS) |
|---|---|---|---|---|
| 100 | 1:0.5 | 180 | 0.3 | |
| 100 | 1:1 | 180 | 0.3 | |
| 100 | 1:2 | 180 | 0.3 | |
| 100 | 1:3 | 180 | 0.3 | |

Table 3. 3 Effect of reaction time on Degree of substitution

| Temperature ( $^0$C ) | Mixing ratio(w/w) | Reaction time(m) | Catalyst loading (%w/w) | Degree of substitution (DS) |
|---|---|---|---|---|
| 100 | 1:3 | 60 | 0.3 | |
| 100 | 1:3 | 120 | 0.3 | |
| 100 | 1:3 | 180 | 0.3 | |
| 100 | 1:3 | 240 | 0.3 | |

Table 3. 4 Effect of Catalyst loading on Degree of substitution

| Temperature ( $^0$C ) | Mixing ratio(w/w) | Reaction time(m) | Catalyst loading (w/w) | Degree of substitution (DS) |
|---|---|---|---|---|
| 100 | 1:3 | 240 | 0.1 | |
| 100 | 1:3 | 240 | 0.2 | |
| 100 | 1:3 | 240 | 0.3 | |
| 100 | 1:3 | 240 | 0.4 | |

### 3.2.4. Preparation of adhesives by using modified starch, PVP and GA

To determine the effects of the PVP, GA, and BA on the bonding strength of adhesive, the one parameter at a time experimental approach was designed as shown in tables 3.5 to 3.8 below to collect the tensile strength as a response.

Table 3. 5 Effect of GA on the tensile strength of the Adhesive formulation at 2 g PVP

| Modified Starch(g) | PVP (g) | GA (g) | BA (g) | Temp($^0$C) | Time (hr.) | Tensile strength(Mpa) |
|---|---|---|---|---|---|---|
| 20 | 2 | 0 | 0.3 | 96 | 2.5 | |
| 20 | 2 | 0.6 | 0.3 | 96 | 2.5 | |
| 20 | 2 | 1.2 | 0.3 | 96 | 2.5 | |
| 20 | 2 | 2 | 0.3 | 96 | 2.5 | |

Table 3. 6 Effect of PVP on the tensile strength of the Adhesive formulation at 2 g GA

| Modified Starch(g) | PVP (g) | GA (g) | BA (g) | Temp ($^0$C) | Time (hr.) | Tensile strength(Mpa) |
|---|---|---|---|---|---|---|
| 20 | 0 | 2 | 0.3 | 96 | 2.5 | |
| 20 | 0.6 | 2 | 0.3 | 96 | 2.5 | |
| 20 | 1.2 | 2 | 0.3 | 96 | 2.5 | |
| 20 | 2 | 2 | 0.3 | 96 | 2.5 | |

### 3.2.5. Lap shear strength test of formulated Adhesive

The tensile strength of the formulated anchote starch-based adhesive was evaluated by measuring the lap shear strength according to the procedures of ASTM D 903-49. The wood specimens were used as the adherend for tensile strength tests throughout this study. The Wood specimens with dimensions of 25 mm (Width), 100 mm (Length), and 4 mm were prepared. These wood pieces were dried using drying oven, and then a constant amount of adhesive slurry (30 mg/cm$^2$) was applied to a 3 cm by 2 cm area of one end of the wood pieces using a brush. Then, the glued woods were allowed to apply a constant load using a C-clamp having the same screw teeth number. Before testing, the lap joints were conditioned for 24 hr. at room

temperature to attain their strength. Finally, the tensile strength (N) of the assembly was measured by a shear strength test using a universal tester machine (WP 310) at a crosshead speed of 2 mm/min for each joint. Then, readings were taken from a computer display. This experiment was done in Wachemo University College of engineering and technology material testing laboratory Lap shear strength ($N/mm^2$) $=\frac{F}{A}$, where F= tensile force (N) and A= adhered area of specimens ($mm^2$). For this specific experiment A= 30 mm * 20 mm = 600 $mm^2$.

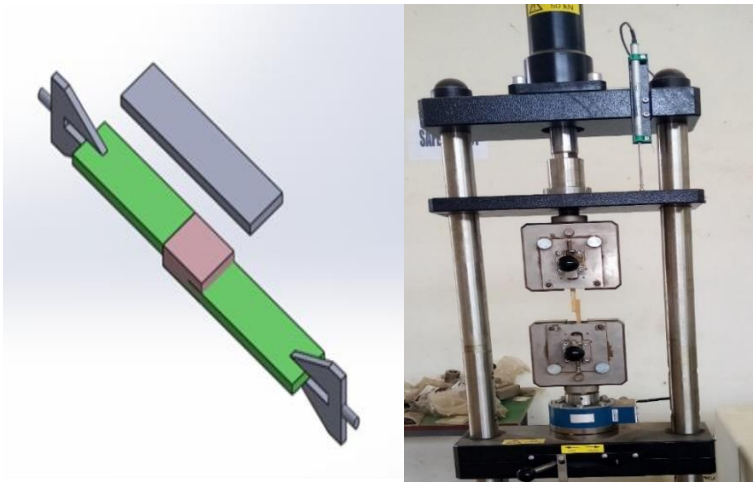

A B

Figure 3. 4 A) Lap joint B) Experimental setup for Lap shear strength test

### 3.2.6. Effect of mixing time, temperature, and cross-linker on lap shear strength

Table 3. 7 Effect Crosslinker on mechanical strength

| Modified Starch(g) | PVP (g) | GA (g) | BA (g) | Temp($^0$C) | Time (hr.) | Tensile strength(Mpa) |
|---|---|---|---|---|---|---|
| 20 | 2 | 2 | 0 | 96 | 2.5 | |
| 20 | 2 | 2 | 0.3 | 96 | 2.5 | |
| 20 | 2 | 2 | 0.6 | 96 | 2.5 | |

Table 3. 8 Effect of mixing time on mechanical strength

| Modified Starch(g) | PVP (g) | GA (g) | BA (g) | Temp($^0$C) | Time (hr.) | Tensile strength(Mpa) |
|---|---|---|---|---|---|---|
| 20 | 2 | 2 | 0.3 | 96 | 1 | |
| 20 | 2 | 2 | 0.3 | 96 | 2.5 | |
| 20 | 2 | 2 | 0.3 | 96 | 3 | |

Table 3. 9 Effect of mixing temperature on Lap shear strength

| Modified Starch(g) | PVP (g) | GA (g) | BA (g) | Temp($^0$C) | Time (hr.) | Tensile strength(Mpa) |
|---|---|---|---|---|---|---|
| 20 | 2 | 2 | 0.3 | 50 | 2.5 | |
| 20 | 2 | 2 | 0.3 | 75 | 2.5 | |
| 20 | 2 | 2 | 0.3 | 96 | 2.5 | |

## 3.3. Characterization

### 3.3.1. Proximate analysis of anchote starch

**Determination of Moisture Content**

The oven was used to determine the moisture content of the starch samples. The crucibles were washed, dried in the oven, and allowed to cool in the desiccator. Then the weight of the crucible was noted ($W_1$). Each starch sample was put in the crucibles and both the crucible and the sample were weighed and registered as ($W_2$). The crucibles containing the samples were then dried in the oven at 105 $^o$C for 3 hours. Finally, the crucibles were taken out and allowed to cool in the desiccator and the weight was noted as ($W_3$). The process of drying, cooling, and weighing continued until constant weight $W_3$ was obtained (AOAC, 1975),

The percentage moisture was calculated as follows:

$$\% \text{ Moisture content} = \frac{\text{Weight lost}}{\text{Weight of sample}} \text{ x } 100 \qquad 3.1$$

$$\% \text{ Moisture content} = \frac{w2-w3}{w2-w1} \text{ x } 100 \qquad 3.2$$

**Determination of Ash Content**

Each starch sample was put in pre-weighed clean and dried crucibles weighting (W1) and the weight of the crucible and the samples was noted as (W2). The crucibles were then transferred into a muffle furnace at 650 $^o$C for 6 hours to burn off the organic matter until grey/white ash was obtained. The crucibles were then removed, allowed to cool in the desiccator and the weights of the crucibles and the ash contents will be noted (W3) (AOAC, 1990).

The ash content was calculated as:

$$\% \text{ Ash} = \frac{\text{weight of Ash}}{\text{weight of sample}} \text{ x } 100 \qquad 3.3$$

$$\% \text{ Ash} = \frac{w3-w1}{w2-w1} \text{x } 100 \qquad 3.4$$

**Determination of Crude Fat**

The fat contents of the samples were determined using the Soxhlet extractor as used by [92]. A known weight of each sample was weighed ($W_1$) on a pre-weighed filter paper weighting ($W_2$), folded neatly and the total weight of the filter paper and the sample was noted ($W_3$). The filter papers, holding the samples were then inserted into the extraction unit and extraction was carried out with petroleum ether (b.pt. 40-60 $^0$C) for 5 hours. After the extraction, the filter papers were removed, dried in the oven at 100 $^o$C for about 30 minutes, allowed to cool in the desiccator, and the weights were noted as (W4). The crude fat percentage was then calculated as:

$$\% \text{ Crude fat} = \frac{\text{Loss in weight}}{\text{weight of sample}} \text{ x } 100 \qquad 3.5$$

$$\% \text{ Crude fat} = \frac{W3-W4}{W1} \text{ x } 100 \qquad 3.6$$

**Amylose content estimation**

The amylose content (%) of the starch was determined by a colorimetric assay using the method described by [93]. The standard stock solution of amylose was prepared by dissolving 0.1 g with 1 mL of ethanol and 9 mL 1 N sodium hydroxide (NaOH) in a 100 mL volumetric flask. The mouth of the flask was covered with a stopper and the contents were mixed well. The samples were boiled for 10 min in a boiling water bath to gelatinize the starch. The samples were removed from the water bath and cooled to room temperature, then fill up to the mark with distilled water and shaken thoroughly. A portion of the stock solution was pipetted into another 100 mL volumetric flask to prepare the standard amylose solutions of 50, 40, 30, 20, and 10%, then 1 mL of 1 N acetic acid and 2 mL of iodine solution (0.2 g I2 and 2.0 g KI in 100 mL of distilled water) were added and made up to volume (100 mL) with distilled water to develop a dark blue color. After 20 min the sample was shaken and the absorbance reading was taken at 600 nm using UV Spectrophotometer (UV-1800, Shimadzu, Japan).

The blank solution contained 1 mL of ethanol and 9 mL of sodium hydroxide was boiled and filled up to the mark with distilled water. Finally, 5 mL was then pipetted into a 100 mL volumetric flask, 1 mL of 1 N acetic acid and 2 mL of iodine solution were added and then filled up to the mark. This was used to standardize the spectrophotometer at 600 nm. Likewise, absorbance readings of the pure amylose solutions of starches were taken at the same wavelengths. The amylose content of starches was estimated from the standard calibration curve

using a relationship between concentrations and absorbance of known mixtures of amylose solutions. The experiment was performed in triplicate and the mean values were taken.

### 3.3.2. Physicochemical characterization native and modified Anchote starch

#### 3.3.2.1. Scanning electron microscopy (SEM) analysis

The morphologies of native anchote starch and modified anchote starches were observed using SEM (Hitachi S-3000N, Tokyo, Japan). Before testing, the samples were mounted on the SEM stubs with double-sided adhesive tapes and then coated with platinum under vacuum to make the sample conductive. Scanning electron photomicrographs were recorded at various magnifications to assure clear images.

#### 3.3.2.2 X-ray diffraction analysis (XRD)

X-ray patterns of native anchote starch and modified anchote starches with different DS values were analyzed between $2\theta = 5°$ and $2\theta = 80°$ using an X-ray diffractometer (Rigaku D/Max-B, Tokyo, Japan) with CuKα radiation at a voltage of 40 kV and 30 mA.

#### 3.3.2.3 Fourier transforms infrared spectroscopy analysis (FTIR*)*

IR spectra of native starch of anchote and modified anchote starches were measured using an FTIR spectrometer (Nicolet Avatar 360, Madison, WI).Samples were diluted at 1:20 with KBr before acquisition. A background of pure KBr was acquired before the sample was scanned. For each spectrum, the DRIFTS was set with an angle of 5° and 128 scans were run.

#### 3.3.2.4 Differential scanning Calorimetry analysis (DSC)

Thermal or gelatinization properties of anchote starches were determined by Differential Scanning Calorimeter (DSC, C30935200187SA, and USA). The technique defined by Abegunde et al.[94], was followed with slight modification. The starch samples (3 g), mixed with distilled water with a ratio of 1:3, starch to distilled water. The mixtures were agitated by a magnetic stirrer at room temperature for 1 h. The sample was quantitatively transferred into DSC pans. Then they were hermetically sealed. The samples were heated from 20 °C to 120 °C at a rate of 10 °C/min. The gelatinization parameters such as onset (To), peak (Tp), conclusion (Tc) temperatures, and gelatinization enthalpy were analyzed and calculated by DSC software.

#### 3.3.2.5. Thermogravimetric analysis (TGA)

Thermogravimetric analyses (TGA) were completed with an instrument calibrated with nickel (Perkin-Elmer TGA, Norwalk, CT). Samples (3–8 mg) were placed in the balance system and heated from 30 to 700°C with a heating rate of 20°C/min in a nitrogen atmosphere. The onset temperature was calculated using TGA software.

### 3.3.3. Characterization of Anchote starch-based adhesive

#### 3.3.3.1. Fourier transforms infrared spectroscopy analysis (FTIR)

IR spectra of formulated adhesive were measured using an FTIR spectrometer (Nicolet Avatar 360, Madison, WI). Samples were diluted at 1:20 with KBr before acquisition. A background of pure KBr was acquired before the sample was scanned. For each spectrum, the DRIFTS was set with an angle of 5° and 128 scans were run

#### 3.3.3.2. Thermogravimetric analysis (TGA)

Thermogravimetric analyses (TGA) were completed with an instrument calibrated with nickel Samples (3–8 mg) were placed in the balance system and heated from 30 to 700°C with a heating rate of 20°C/min in a nitrogen atmosphere. The onset temperature was calculated using TGA software

# CHAPTER FOUR

# 4. RESULT AND DISCUSSIONS

## 4.1. Physicochemical characterization of Anchote starch

### 4.1.1. Proximate analysis of native anchote starch

The proximate analysis (moisture content, crude protein, crude fat, and ash content) of anchote starch is shown in Table 4.1. The ash content is the residue after the complete combustion process of carbon-free compounds, like minerals and inorganic salts in the fresh tuber, fertilizer use, and can also come from the soil and air contamination during processing. In this work, anchote starch had ash content slightly greater than previously reported work [23]. This higher value indicates that anchote starch had more inorganic compounds like calcium (Ca), iron (Fe), phosphorous (P) relative to other root tubers like potato, sweet potato, and cassava [95]. The crude fat content in anchote starch was 0.56% which was relatively higher than previously stated work[23]. This may be depends on different determining methods of Pearson et al (1981) and the AOAC (2006) official [23]. The moisture content of anchote starch in this work was (9.506 ± 1.25%) which is almost the same previously reported work of [23]. The amylose and amylopectin content of anchote starch is slightly different from previously reported[93]. In the estimation of amylose content, amylose solutions, as well as their mixtures stained with iodine solution, showed a linear relationship between absorption and concentration at 600 nm. According to the standard linear curve equation [$A = 0.0166X + 0.054$; $R2 = 0.9995$; where A is absorbance value, X is concentration of amylose (%)], the amylose contents of the anchote starches was estimated to be 28 % as show in Table 4.1

Table 4. 1 Proximate analysis of anchote starch

| Sample | Crude fat (%) | Ash (%) | Moisture (%) | Amylose Content | Amylopectin Content |
|---|---|---|---|---|---|
| Anchote starch | 0.56 ± 0.05 | 0.6 ± 0.244 | 9.506 ± 1.2 | 28 | 72 |
| Previously reported | 0.2.0 ± 00 | 0.30 ± 0.00 | 9.06 ±0.11 | 32 | 68 |

Data (mean ± SD) at ($P \leq 0.05$)

### 4.1.2. Morphological analysis of native anchote starch

The morphological characteristics of anchote starch granules were determined by using SEM. The SEM images in Fig 4.1. Shows the morphological characteristics of anchote starch granules. The observed microscopic appearance of anchote starch granules shape is slightly different from the previously done literature. From SEM results, anchote starch granules were dome-shaped with polygonal and some with granules with irregular shapes. This is because the morphology of the starch granules is affected by the physiology of the plant, biological origin of the plant [96]. The anchote starch granules size, mean width, and length are tabulated as follows.

Table 4. 2 Anchote, starch granule size.

| Sample | Mean granule width (μm) | Width range (μm) | Mean granule length (μm) | Length range (μm) |
|---|---|---|---|---|
| Anchote starch | 9.23 | 2.21–16.26 | 11.57 | 3.15–19.99 |

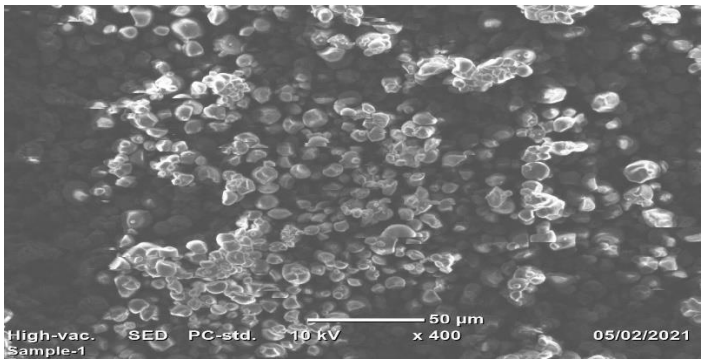


Figure 4. 1 SEM images of Anchote starch

### 4.1.3. Crystallinity analysis of native anchote starch

The crystalline polymorphs of native anchote starch were observed by X-ray diffraction. Fig 4.2. Below shows the x-ray diffraction pattern of anchote starches. The diffraction patterns provide information on the arrangement of the amylopectin chain in double helices. The x-ray pattern of starch has been classified as A-type, B-type, and C-type starches.

A-type starch is typical for cereals starches have a doublet at around 17° and 18° of 2θ and present strong diffraction peaks about 15° and 23° of 2θ. B-type is typical for in tubers starches and patterns identified by a strong peak at 17° of 2θ and a characteristic peak about 5.6°, 15.26°, 17.21°, 19.75°, 22.32° and 24.08° of 2θ. In addition to these peaks, it has weak diffraction peaks at 2θ = 5.81° and 26.10°. C-type starch patterns are a combination of A-type starch and B-type starch. The characteristic diffraction peaks of type C starch were observed at 2θ = 15.06°, 17.09°, 19.34° and 22.86° [23, 97]. Anchote starch showed strong diffraction peaks at 17° of 2θ with characteristics peak at 5.6°, 15.26°, 17.21°, 19.75°, 22.32° and 24.08° of 2θ. According to these diffraction peaks, anchote starch is a B-type starch

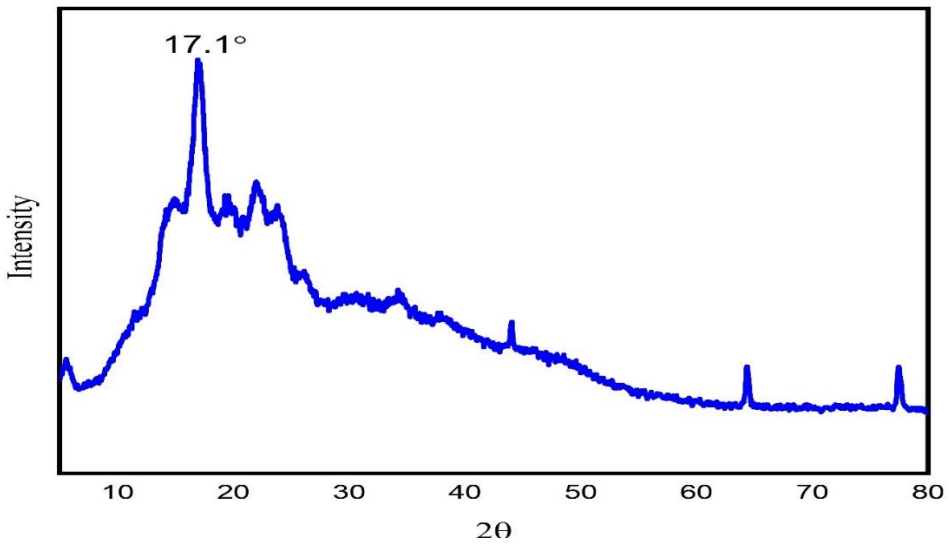


Figure 4. 2 X-ray diffraction of anchote starch

### 4.1.4. Thermal property analysis of native anchote starch

#### 4.1.4.1. Differential scanning Calorimetry (DSC)

The DSC thermograms of anchote starches analyzed at a starch-distilled water ratio of 1:3 and data from the gelatinization endothermic curve and gelatinization temperature are provided in table 4.3 below. These gelatinization temperatures are classified as onset (To), peak (Tp), and

conclusion (Tc). Gelatinization is a process in which starch granules change their semi-crystalline structure into an amorphous state. This transformation is attained by heating starch in the presence of distilled water. The onset temperature is the temperature when samples begin to gelatinize, whereas the maximum intensity of gelatinization occurs at peak temperature and conclusion temperature is the temperature where gelatinization concludes[23]

The thermograms of anchote starch were the onset temperature is 72.54 °C, the peak temperature is 79.94 °C, and the conclusion temperature is 84.87 °C respectively. Anchote starch exhibited significantly higher gelatinization onset temperature as compared to anchote starch which was previously reported as 68.94 °C[93]. These temperatures directly relate to the degree of the arrangement of the molecules in starch granules[98]. Starch composition and architecture of crystalline/amorphous regions have been known to influence the degree of gelatinization. Based on these observations, it can be concluded that this anchote starch has higher crystallinity than previously reported [23] anchote starch. This may be associated with the botanic origin or environmental condition on which raw anchote plant grown.

Table 4. 3 Thermal characteristics of anchote starches

| Sample | $T_0$ ($^0$C) | $T_P$ ($^0$C) | $T_C$ ($^0$C) | $T_C$-$T_0$ ($^0$C) | ΔH (J/g) |
|---|---|---|---|---|---|
| Anchote starch | 72.54 | 79.94 | 84.87 | 12.33 | 13.35 |

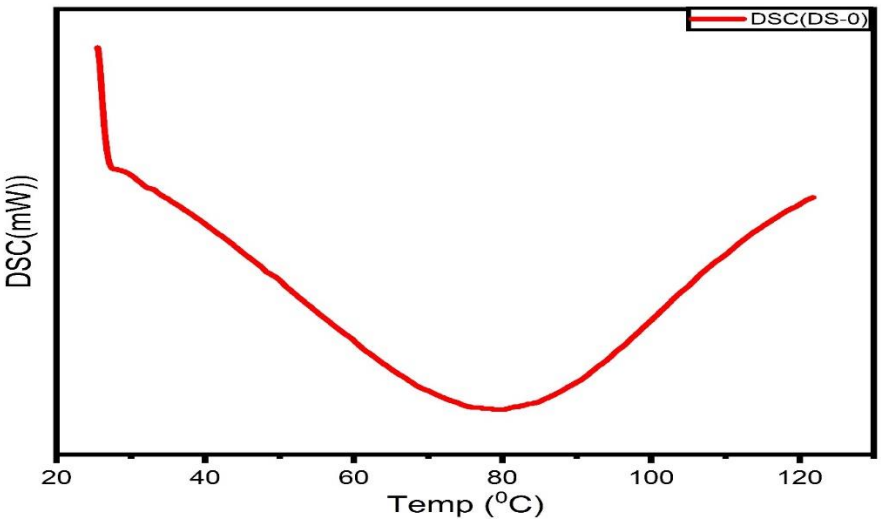


Figure 4. 3 DSC curve of native anchote starch

#### 4.1.4.2. Thermogravimetric analysis (TGA)

The thermal stability of the Anchote starch was evaluated using thermogravimetric analysis (TGA). TGA results of anchote starch are presented in Figure 4.4 below. Generally, weight loss occurred in three sections. The first weight loss (10.15%) was observed in the 29 –128 ℃ temperature range and it is attributed to the release of physically adsorbed, volatile components and hydrogen-bonded water that remained in starch even after preconditioning. The second weight loss (55.15%) took place in the 241–321 ℃ temperature range and was assigned to starch decomposition. As shown in the DTG curve in Fig 4.4, the highest decomposition occurred in the range of 241–321 ℃. The decomposition of starch is a result of inter and intramolecular dehydration reactions of starch molecules, with water as a main product of decomposition. The third weight loss (34.7%) took place in the temperature range of (321-611 ℃) resulted in carbonization and ash formation from decomposed monomers.

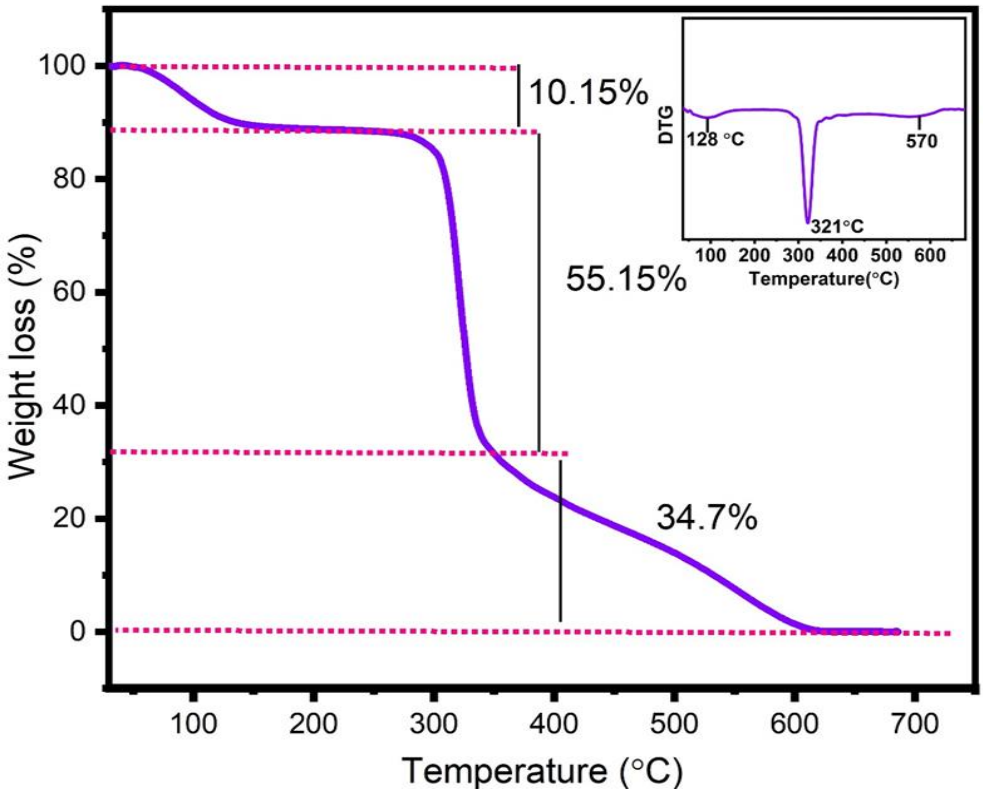


Figure 4. 4 TGA curves of native (DS-0) anchote starch

### 4.1.5. FTIR analysis of Native anchote starch

The Fourier Transform Infrared Spectroscopy (FTIR) spectra of anchote starch are presented in Fig 4.5 below. This starch showed different bands due to vibrational modes of amylose and

amylopectin structures [93]. The broad bands observed at (3010-3600) $cm^{-1}$ for anchote starches indicate the stretching vibrations of O-H groups[99]. The peak at 2930 $cm^{-1}$ for Anchote starch represents the Stretching vibration of C-H in $CH_2$ [100]. The peak at 1647 $cm^{-1}$ for anchote starch indicates O–H bending vibration of adsorbed water molecules of H–O–H [101]. The peaks at 1411 $cm^{-1}$ for anchote starch are associated with $CH_2$ symmetric deformation and the peaks 1366 $cm^{-1}$ are associated with C -H symmetric bending. The absorption band at 1204,1079 and 1153 $cm^{-1}$ for anchote starch was assigned to the coupling of C–O, O–H, and C–C bonds[93]. The absorption peaks at 1153,1079 and 1024 $cm^{-1}$ for anchote starches were believed to be due to the C–O bond stretching from the anhydrous glucose ring[58]. There are several additional characteristics absorption peaks at 930, 856, 761, 708, 670, 650, 617, 583, 571, and 529 $cm^{-1}$ are associated with C-O-C anhydroglucose at α-1,4 glycosidic linkage ring stretching vibrations [101, 102] as shown in table 4.5 below

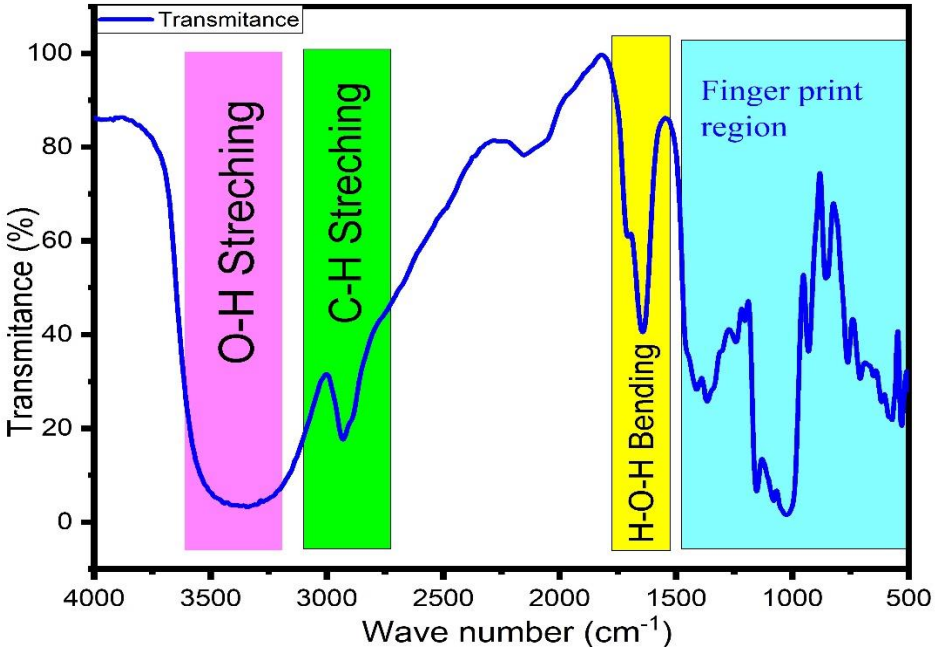


Figure 4. 5 FT-IR spectra of anchote starches

Table 4. 4 Band assignment of anchote starches

| Functional group | Wavenumber ($cm^{-1}$) from literature | Anchote starch maximum peak ($cm^{-1}$) | Reference |
|---|---|---|---|
| O - H stretching | 3010-3600 | 3439 | [101] |
| C - H stretching | 2931 | 2930 | [57] |
| O–H bending vibration of adsorbed water molecules of H–O–H | 1647 | | [101] |
| O = C = O | 2150 | 2153 | [100] |
| $CH_2$ symmetric scissoring | 1415 | 1411 | [100] |
| C -H symmetric bending | 1385-1375 | 1366 | [100] |
| C - O - C asymmetric stretching | 1149 | 1153 | [100] |
| C - O stretching | 1250 – 800 | 1242,1204,1153,1079,1024,930, and 856 | [100] |
| C - O - C ring vibration of carbohydrate | 920, 856, 758 | 930, 856, 761, 708, 670, 650, 617, 583, 571, and 529 | [102] |

## 4.2. Modification/Acetilazation of starch

Acetylation of starch is the conversion of three available hydroxyls (O-H) groups to acetyl groups by substitution[103]. It is the most common and basic method that the starch reacted with long-chain organic acids such as anhydrides by using different kinds of catalysts. The focus point of this study was the Acetilazation reaction of starch with acetic anhydride with NaOH catalyst. AS shown in Fig 4.6 and Fig 4.7 below, during the reaction of starch with acetic anhydride by using NaOH catalyst the Nucleophilic substitution at an unsaturated carbon atom of acetic anhydride substituted by an addition-elimination reaction mechanism. As shown in the figure below, one glucose molecule has three free O-H groups with different reactivates. The

primary O-H on $C_6$ is more reactive and is acetylated easily than the secondary ones on $C_2$ and $C_3$ due to steric hindrance. The reactivity of the three free OH groups of the glucose decreases in the following order during starch acetylation: primary C (6) O-H > secondary C (2) O-H > secondary C (3) O-H.

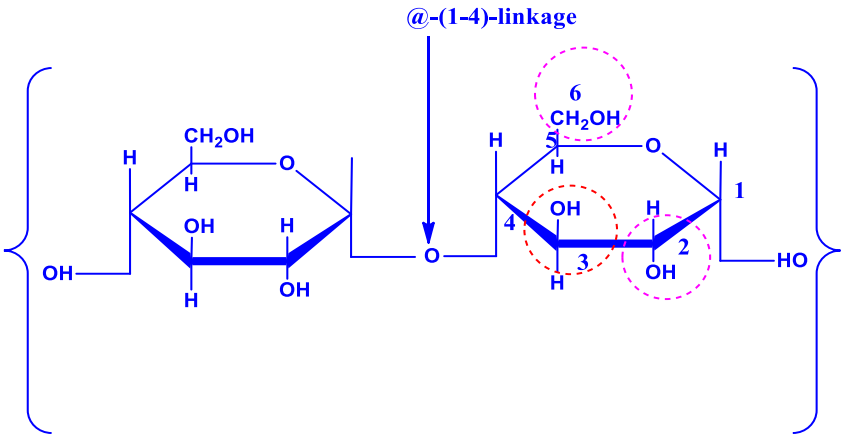


Figure 4. 6 Linear/amylose structure of starch

Location of hydroxyl groups within the interior surface of starch forming hydrogen bonds with the O-H groups on the neighboring glucose units, make these hydroxyl groups less accessible for acetic anhydride, justifying the incomplete acetylation even at high catalyst and acetic anhydride concentrations[101]

It is known Acetylation can improve shortcomings like hygroscopicity, brittleness, sensitivity to enzymes and acids, insolubility in organic solvents, flexibility, hydrophobicity, and processability by altering the structure and affecting the hydrogen bonding of amylose and amylopectin in a manageable method to enhance and extend starch applications [103, 104]. The introduction of acetyl groups disturbs the ordered structure of native starch and interferes with the re-association of amylose and amylopectin in gelatinized starch, leading to the change in morphological properties, crystalline properties, gelatinization properties, and gelatinization enthalpy of the starch. The changes of anchote starch before and after acetilazation with different degrees of substitution (DS) were investigated by FTIR, SEM, DSC, TG–DTG, and XRD as follows.

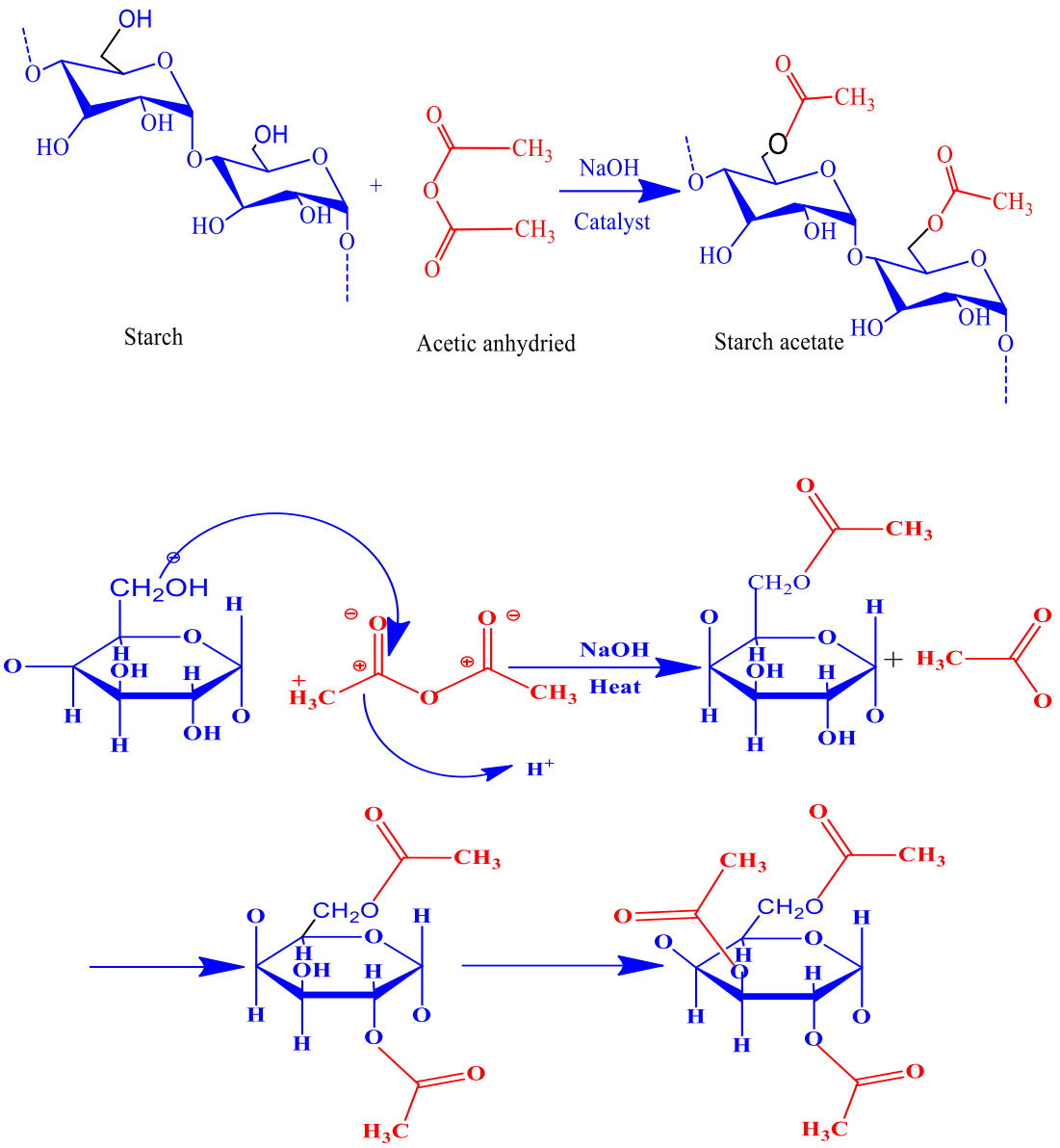


Figure 4. 7 Reactions mechanism of starch and acetic anhydride

### 4.2.1. FTIR analysis of Modified starch

FTIR spectroscopy was used to validate the change in the chemical structure of the anchote starch molecules associated with the acetylation reaction of starch and acetic anhydride. To detect the structure of acetylated starches and the spectra of the native starch, DS- 0.0, DS- 0.54, DS-1.49, DS-2.26, and DS-3.00 acetylated starches are shown in Fig. 4. 8. In the spectra of native anchote starch Fig 4.8. (a), there are several clear absorbencies at 3439,2930, 2153, and 1647 cm-1 represents the stretching vibrations of O-H groups[99], the Stretching vibration of C-H in $CH_2$,Stretching of O=C=O[100], and O–H bending vibration of adsorbed water molecules of H–O–H [101] respectively.

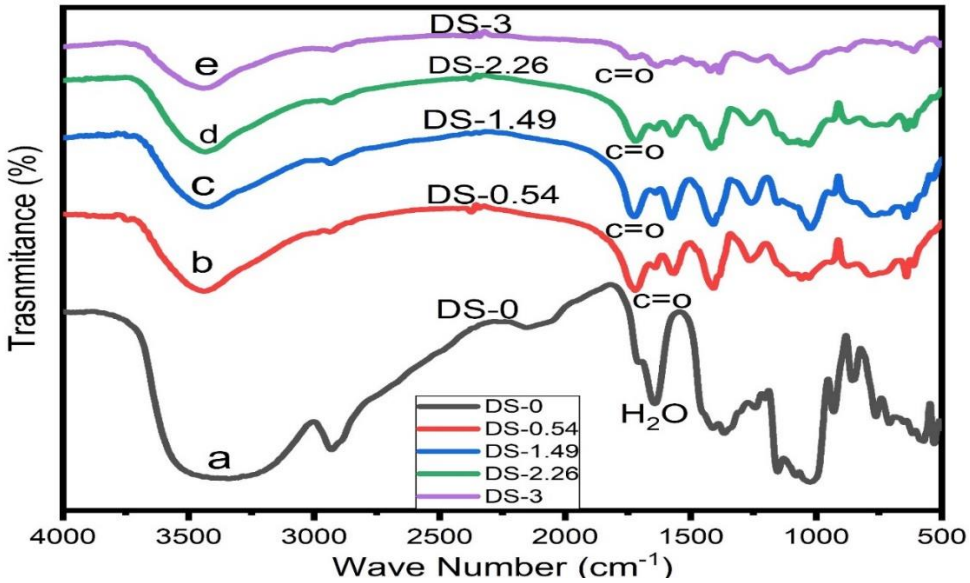


Figure 4. 8 FTIR spectra of DS-0, DS-0.54, DS-1.49, DS-2.26 and DS-3.00

The peaks at 1411 $cm^{-1}$ for anchote starch are associated with $CH_2$ symmetric deformation and the peaks 1366 $cm^{-1}$ are associated with C -H symmetric bending. The absorption band at 1204,1079 and 1153 $cm^{-1}$ for anchote starch was assigned to the coupling of C–O, O–H, and C–C bonds[93]. The absorption peaks at 1153,1079 and 1024 $cm^{-1}$ for anchote starches were believed to be due to the C–O bond stretching from the anhydrous glucose ring[58]. There are several additional characteristics absorption peaks at 930, 856, 761, 708, 670, 650, 617, 583, 571, and 529 $cm^{-1}$ are associated with C-O-C anhydroglucose at α-1,4 glycosidic linkage ring stretching vibrations [101, 102].

As shown in Fig.4.8.(b),(c),(d), and (e), FT-IR spectra of different DS -0.54, DS-1.49,DS-2.26 and DS- 3 of acetylated starches showed some new absorption at 1739, 1435, 1335, and 1239 $cm^{-1}$ assigned to carbonyl C=O, $CH_3$ antisymmetric deformation vibration, and $CH_3$ symmetry deformation vibration and carbonyl C–O stretch vibration, respectively. The appearance of these new absorption peaks confirms the formation of the acetylated starch, a product of the esterification reaction[57]. The intensity of those bands increased with the esterification level, whereas the intensity of the band assigned to the stretching of hydroxyl groups (O-H) of starch (3439 $cm^{-1}$) progressively decreased as a result of the increasing number of hydroxyls which were replaced by ester groups. Also, a noticeable decrease of the absorbance peaks at 1024, 1079, and 1153 $cm^{-1}$, characteristic of the C–O stretching of the native starch observed, as the hydroxyl groups were replaced by the ester group[57, 101].

### 4.2.2 Thermogravimetric analysis (TGA)

Thermogravimetric analyses (TGA) curves were used to see the change of thermal stability caused by the acetylation of starch and to determine the weight loss of the starch on heating. The TGA and DTG curves for the native (DS-0) anchote starch and starch acetates with different DS were shown in Fig.4.9 and Fig.4.10. Generally, weight loss occurred in three sections. The first weight loss (10%) was observed in the 29 –128 ℃ temperature range and it is attributed to the release of physically adsorbed, volatile components and hydrogen-bonded water that remained in starch even after preconditioning[105]. The second weight loss (55.15%) took place in the 128–321 ℃ temperature range and was assigned to starch decomposition. As shown in the DTG curve in Fig 4.10, the highest decomposition occurred in the range of 128–321 ℃, and the temperature of maximum weight loss rate ($T_{max}$) of native starch occurred at 321℃ as calculated from DTG data. $T_{max}$ indicates the point of the greatest rate of change on the weight loss curve. The decomposition of starch is a result of inter and intramolecular dehydration reactions of starch molecules, with water as a main product of decomposition. The third weight loss (34.7%) took place in the temperature range of (321-611 ℃) resulted in carbonization and ash formation from decomposed monomers.

As shown in Fig.4.9 and Table 4.5 10% weight loss of native starch (DS-0) occurred at 159 ℃, 50% weight loss at 326 ℃, 90% weight loss at 540 ℃ and maximum degradation temperature ($T_{max}$) occurred at 321 ℃. For modified starch (DS-0.54), 10% weight loss occurred at 122 ℃, 50% weight loss occurred at 283 ℃, 90% weight loss occurred at 376 ℃ and maximum degradation temperature ($T_{max}$) occurred at 298 ℃. In general, esterification of starch has been reported to result in increased thermal stability, which is characterized by a single DTG peaks that occur at higher temperatures than the one found for native starch decomposition. For esterified starch (DS-0.54) thermal stability decreased in opposite to general esterification principles as shown in Fig.4.10.and Table.4.5. The maximum degradation temperature for esterified starch (DS-0.54) was (Tmax =298℃) which is less than the maximum degradation temperature of native starch (DS-0) ($T_{max}$ =321℃) when DS increased from 0 to 0.54. This may be due to the occurrence of a free O-H group on esterified starch due to incomplete substitution of acetyl group during esterification modification and appearance of impurities like unreacted acetic anhydride. It is believed that free OH and unreacted acetic anhydride catalyzes the decomposition of esterified starch under lower temperatures.

Also, as shown in Fig.4.9 and Table.4.5 10% weight loss of modified starch (DS-1.49) occurred at 132 ℃, 50% weight loss at 274 ℃, 90% weight loss at 366 ℃ and the maximum degradation temperature ($T_{max}$) occurred at 302 ℃. For modified starch (DS-2.26),10% weight loss occurred at 145 ℃,50% weight loss occurred at 283 ℃,90% weight loss occurred at 366 ℃ and the maximum degradation temperature($T_{max}$) occurred at 312 ℃. As modified starch (DS-0.54), also these modified starch samples with DS-1.49 and DS-2.26 show low thermal stability compared to native starch (DS-0). This is confirmed by their maximum degradation temperature ($T_{max}$) that means $T_{max}$ (DS-1.49) = 302 ℃ < $T_{max}$ (DS-2.26) = 312 ℃ < $T_{max}$ (DS-0) is 320 ℃. This less thermal stability related with free OH group on esterified starch of two samples due to incomplete substitution of acetyl group during esterification modification and appearance of impurities like unreacted acetic anhydride.

On other hand, as shown in Fig.4.9 and Table.4.5 For modified starch with DS-3, 10% weight loss occurred at 232 ℃,50% weight loss occurred at 344 ℃,90% weight loss occurred at 479 ℃ and the maximum degradation temperature($T_{max}$) occurred at 362 ℃. In this case, the $T_{max}$ of modified starch with DS-3 is 362 ℃ which is much greater than the $T_{max}$ of native starch (DS-0) which is 320 ℃. This result confirms that the modified starch sample with DS-3 was thermally more stable than native starch (DS-0). The increase in thermal stability was due to the low amount of remaining hydroxyl groups (OH) in starch molecules after modification. The increase in molecular weight and covalent bonding due to the acylation of hydroxyl groups(OH) was also responsible for the increased thermal stability[106].

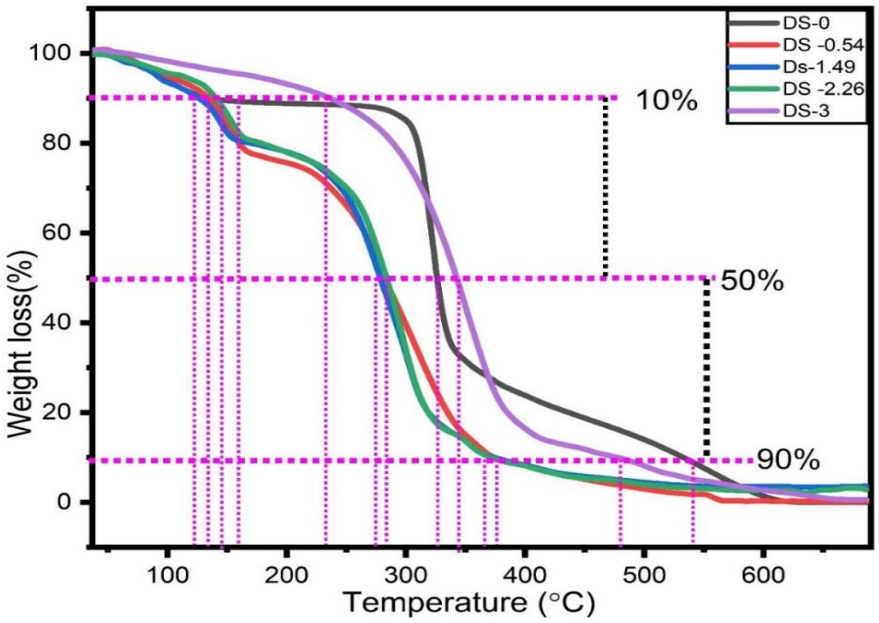


Figure 4. 9 TGA curves of (DS-0, DS-0.54, DS-1.49, DS-2.26, and DS-3

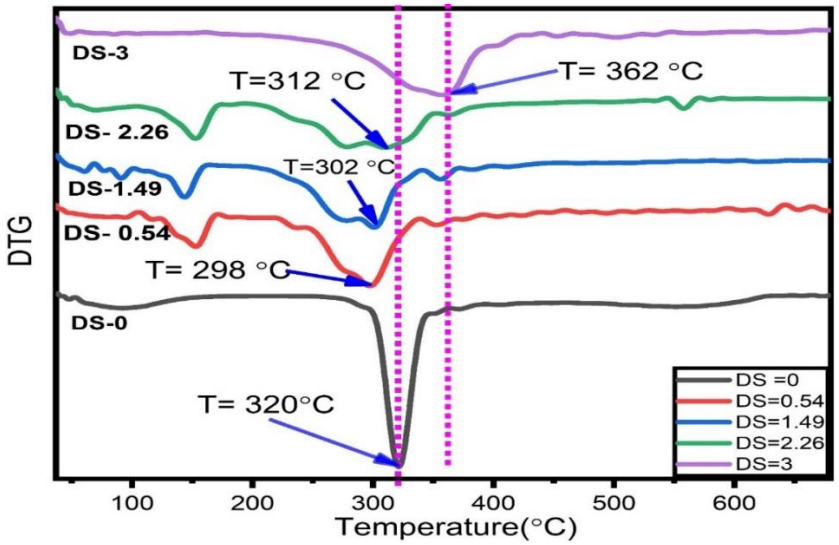


Figure 4. 10 DTG curves for (DS-0, DS-0.54, DS-1.49, DS-2.26, and DS-3)

Table 4. 5 TGA analysis of different DS weight loss and maximum degradation.

| Sample | $T_{10\%}$ ($^0$C) | $T_{50\%}$ ($^0$C) | $T_{90\%}$ ($^0$C) | $T_{max}$ ($^0$C) |
|---|---|---|---|---|
| DS-0.00 | 159 | 326 | 540 | 320 |
| DS-0.54 | 122 | 283 | 376 | 298 |
| DS-1.49 | 132 | 274 | 366 | 302 |
| DS-2.26 | 145 | 283 | 366 | 312 |
| DS-3.00 | 232 | 344 | 479 | 362 |

### 4.2.3. Starch granule morphology

The scanning electron micrographs (SEM) of native anchote starch (NAS) and acetylated anchote (AAS) are presented in Fig.4.11 SEM investigations show that acetilazation can change the structure of starch granules significantly, compared with NAS. NAS granules are smooth, roughly polygonal in shape, ranging from 1.31 to 17.26 μm in average width and 3.35–18.09 μm in average length in Fig 4.11(a). Fig.4.11 (b) shows the microphotograph of AAS with a high DS (DS-3). The morphology of the starch granule shows a clear external structural difference between NAS and AAS. Additionally, the starch granules start to rupture and different sizes of cracks are formed on their surfaces when acetilazation takes place. These eroded surface appearances are observed to be less smooth than NAS. The morphological variations in AAS granules become more different in their shape and size with high DS (DS-3) as shown in Fig.4.11 (b). It also can be seen from Fig. 4.11(b) that there are no integrated starch granules detected and the interior of starch granules are also susceptible to the acetilazation process takes place. SEM pictures of AAS clearly show (Fig.4.11 b) that the AAS with DS-3 has been more easily affected by the introduction of acetyl groups. Therefore, the above results show that the external, as well as internal parts of the starch granules, are influenced by the chemical acetilazation processes, which means that the crystallinity of the starch decreases slightly. The introduction of acetyl groups brought significant changes in the shapes and the sizes of the starch granules which occur not only in some surface modification.

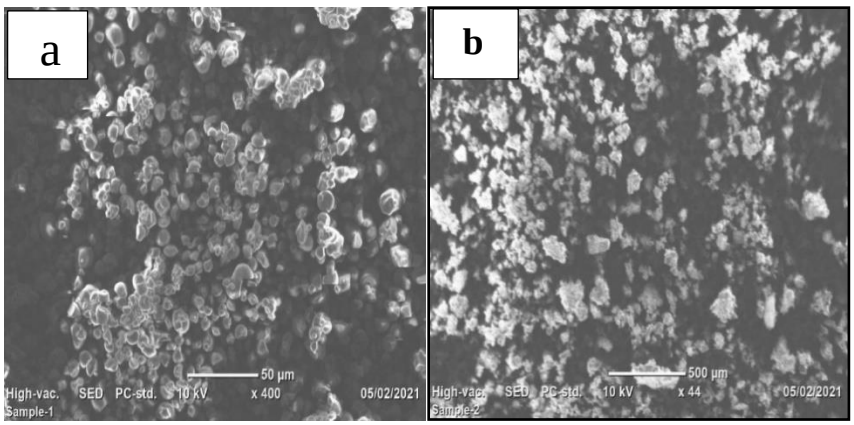


Figure 4. 11 Morphology of (a) native (DS-0) and (b) modified (DS-3) anchote starch

### 4.2.4. Differential scanning Calorimetry (DSC)

Gelatinization properties of native and acetylated anchote starches as measured by differential scanning calorimetry (DSC) are summarized in Table 4.6 Modified anchote starches showed noticeable differences in their thermal behavior, both with each other as well as to the native starch as shown in Table 4.6 After acetylation of starch, the To, Tp, and Tc and ΔH values were decreased, whereas the gelatinization temperature range (Tc-To) was increased when the degree of substitution increased from DS-0 to DS-3. The decrease in the gelatinization temperatures after acetylation modification have been reported in previous studies[107-109] and characterize the weakening of the granules after the introduction of acetyl groups, which leads to premature rupture of double helices of amylopectin during heating[109]. Gelatinization temperature and enthalpy of modified starch decreased relative to native starch with increasing the degree of substitution. As shown in Fig.4.12 and Table.4.6 a gelatinization temperature of native (DS-0) anchote starch decrease from ($T_O$ = 72.54 °C) to ($T_O$ = 60 °C) by acetylation (DS-3). In the same scenario Peak temperature ($T_P$) and conclusion temperature ($T_C$) of native starch (DS-0) decreased from 79.94 and 84.87 $^0$C to 56.96 and 70.49 (DS-3). The enthalpy of native starch (DS-0) was 42.42 J/g which decreased to 2.35 J/g when starch-modified (DS-3). Enthalpy is the latent heat absorbed by the melting of crystallites in the granules, which depends on different factors such as crystallinity, intermolecular bonding, rate of heating of starch suspension[110]. A decrease in temperature and enthalpy of gelatinization may be related to the reduction of crystallinity of acetylated starches, as observed by XRD results[109]. The value of enthalpy reflects the loss of the ordered structure of double helices as well as changes in the starch crystallinity. Higher gelatinization temperature is related to starches with a high degree of

crystallinity, which provides structural stability to the granules and higher resistance to gelatinization. Starches with higher amylose content have an amorphous region, and their crystalline structure is lost at lower gelatinization temperatures[107].

Table 4. 6 Thermal properties of native and acetylated anchote starches

| Modification | DS | Gelatinization temperature | | | Enthalpy(J/g) |
|---|---|---|---|---|---|
| Acetilazation | | $T_O$ ($^0$C) | $T_P$ ($^0$C) | $T_C$ ($^0$C) | |
| | DS-0 | 72.54 | 79.94 | 84.87 | 42.42 |
| | DS-0.54 | 56.24 | 58.49 | 72.09 | 39.46 |
| | DS-1.49 | 54.24 | 58.32 | 72.06 | 35.18 |
| | DS-2.26 | 52.63 | 57.24 | 71.33 | 30.71 |
| | DS-3 | 51.55 | 56.96 | 70.49 | 2.35 |

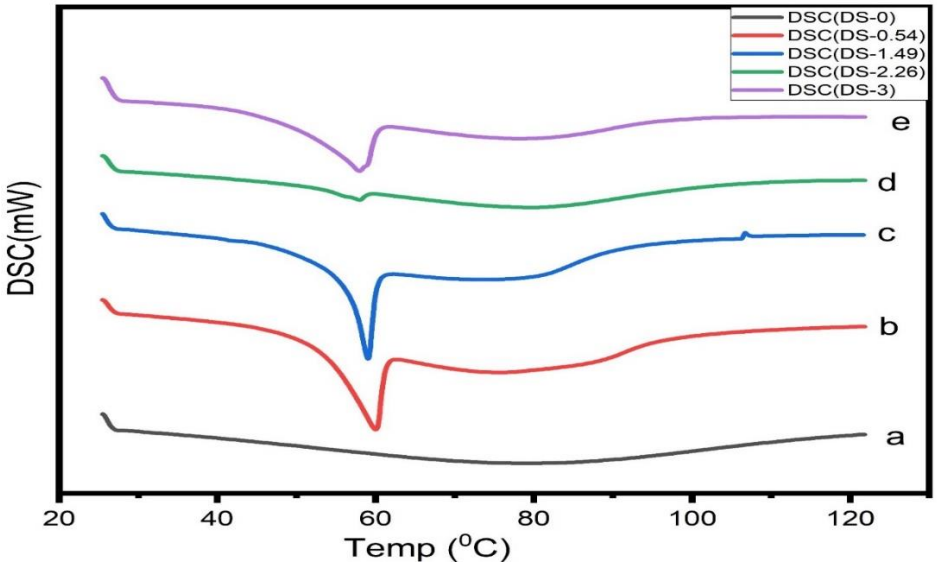


Figure 4. 12 DSC of (DS-0) and (DS-0.54, DS-1.49, DS-2.26, and DS-3)

### 4.2.5. XRD analysis of Modified starch

X-ray diffraction (XRD) measurements were done to check if acetylation changed the crystallinity of starch. The X-ray diffraction spectra of native anchote starch and acetylated anchote starches are presented in Fig.4.13 below. The native anchote starch had sharp diffraction peaks at 17° (2θ) and a few characteristics peaks at 5.6°, 15.26°, 17.21°, 19.75°, 22.32°, and 24.08°, which indicated a typical B-type pattern[23, 108]. As can be seen in Fig.4.13, DS-0.54 acetylated starch showed a similar structural profile to the native one(DS-0), but it had a new

peak at 11° (2), which appeared diffusion peaks of acetylated starch[111]. However, DS-1.49 and DS-2.26 acetylated starch represented typical peaks of acetylated starches, which had sharp peaks at 9° and 29° (2θ) and at DS-3 acetylated starch all sharp peaks were disappeared as shown in Fig.4.13. These X-ray diffraction(XRD) results indicated that with esterification modification, the crystalline structure of native starch was damaged and new structure of acetylated starch was formed [99]. As a result, the degrees of crystallinity decreased with increasing the DS from DS-0 to DS-3. This is due to intra- and inter-molecular hydrogen bonds were responsible for the highly ordered crystalline structure [106, 112]. During the esterification modification process, acetyl groups substituted some of the hydroxyl groups on starch, this reduces the formation of intermolecular hydrogen bonds and thereby destroying the ordered crystalline structure [109]. As the DS of the starch acetate increased from DS-0 to DS-3, there was increased destruction or even loss of the ordered crystalline structure[58].

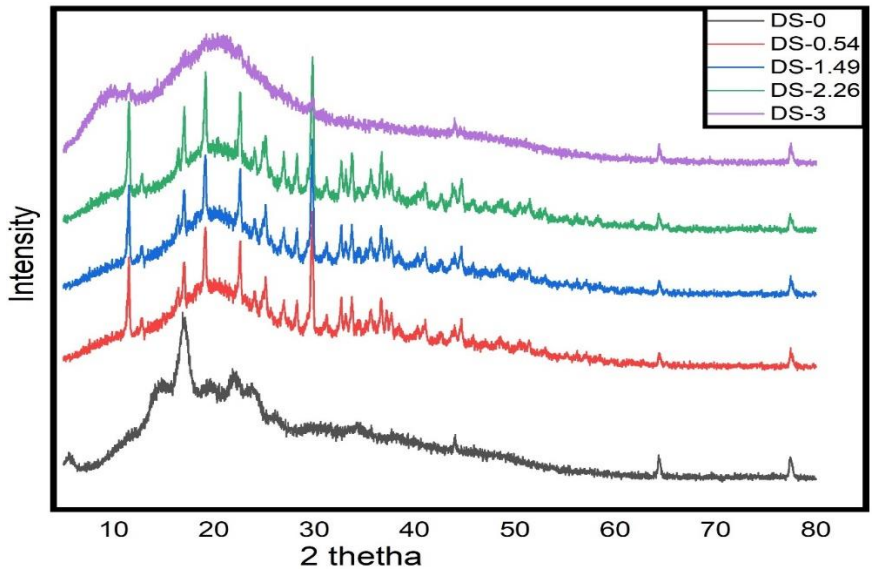


Figure 4. 13 XRD of (DS-0, DS-0.54, DS-1.49, DS-2.26, and DS-3)

## 4.3. Determination of degree of substitution (DS)

### 4.3.1. Effect of temperature on DS

To investigate the acetilazation extent of anchote starch at the specified reaction temperatures, the gelatinization temperature must be known since no reaction will takes place below the gelatinization point. Previously reported gelatinization temperature of anchote starch for onset, peak, and conclusion temperatures were 66.58 °C, 70.18 °C, and 73.98 °C, respectively [23]. In this research, the reaction temperature was selected to be in the range of 80–100 $^{0}$C based on

affirmation of gelatinization temperature. The effect of reaction temperature on degree of substation is presented in Table 4.7 for reaction conditions of catalyst loading (0.3 g/g), maxing ratio (1:3 g/g), reaction time (180 min). An increment in the DS was observed when the temperature increases from 80 to 100 $^0$C, leading to the formation of starch acetates with DS values ranging from 1.52 ± 0.3 to 2.03± 0.01. This phenomenon can be correlated with high swelling ability and diffusion rate of acetic anhydride in to the starch matrix arises due to the temperature increment up to 100 $^0$C. However, it is well known fact on the literature that the DS used to decreases as the temperature increases beyond the degradation temperature of the starch which can be further observed as a darker color of the matrix. These results were confirmed by FTIR analysis as shown in Fig.4.14 below.

Table 4. 7 DS values measured by titration for different reaction temperature

| Temperature (℃ ) | Mixing ratio(w/w) | Reaction time (min) | Catalyst loading (g/g) | DS |
|---|---|---|---|---|
| 80 | 1:2 | 180 | 0.3 | 1.52 ± 0.3 |
| 85 | 1:2 | 180 | 0.3 | 1.71 ± 0.2 |
| 90 | 1:2 | 180 | 0.3 | 1.90 ± 0.04 |
| 100 | 1:2 | 180 | 0.3 | 2.03 ± 0.01 |

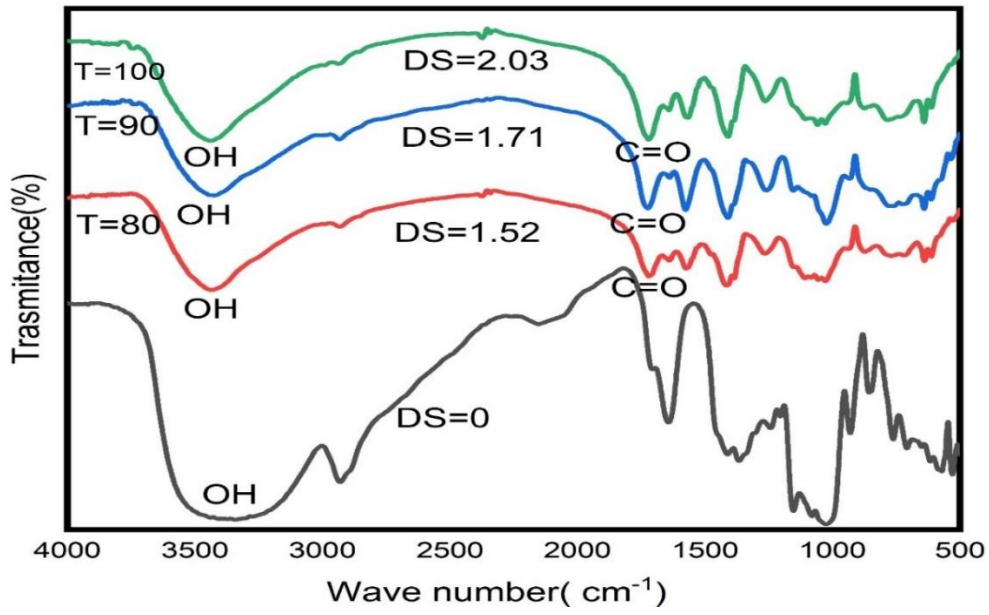


Figure 4. 14 Effect of temperature on FTIR Spectra of native and modified starch

Additionally, lower values of DS (<0.2) is observed for a temperature below 80 $^0$C. Even though the starch acetate with lower DS values cannot be used as an input for adhesive, Food and Drug Administration (FDA, USA) approved DS ranging from 0.01–0.2 to improve binding,

thickening, stability, and texturizing of the food industry[99, 111]. Based on this the reaction temperature below 80 $^{0}$C is suitable for anchote starch modification for food applications. Highly acetylated starch with a degree of substitution (DS) of 2.00–3.00 was the interest this research for their solubility (within acetone and chloroform) and thermoplasticity [112, 113]. The moderate and highly esterified starches are candidates for engineered materials with suitable mechanical characteristics compared with native[114]. As a biodegradable carbohydrate polymer material, acetylated starch also has many potential uses in hot melt adhesives, coatings, cigarette filters, biodegradable packaging materials, tablet binders, and other pharmaceutical applications[115]. With this it can be concluded that the acetylated anchote starch can be applied in different potential applications and used as an input in different kinds of industries.

### 4.3.2. Effect of acetic anhydride concentration (mixing ration) on DS

As shown in Table 4.8 below, the effects of the ratios of acetic anhydride to starch or concentration of acetic anhydride (AH/S), increased from 0.5 to 3 as DS increased from 0.13 ± 0.4 to 2.26 ± 0.3. This is because the increment of acetic anhydride concentration resulted in a high molecular collision rate and greater availability of acetic anhydride molecules in the around of starch granules. The immobility of the hydroxyl groups made this acetylation reaction principally dependent on the availability of acetic anhydride molecules in the proximity of the starch molecules [55, 101, 116]. This result is also confirmed by FTIR analysis as shown in Fig.4.15 below

Table 4. 8 DS values measured by titration for different acetic anhydride concentration

| Temperature (℃) | Mixing ratio(w/w) | Reaction time (min) | Catalyst loading (g/g) | DS |
|---|---|---|---|---|
| 100 | 1:0.5 | 180 | 0.3 | 0.13 ± 0.4 |
| 100 | 1:1 | 180 | 0.3 | 0.54 ± 0.06 |
| 100 | 1:2 | 180 | 0.3 | 1.49 ± 0.1 |
| 100 | 1:3 | 180 | 0.3 | 2.26 ± 0.3 |

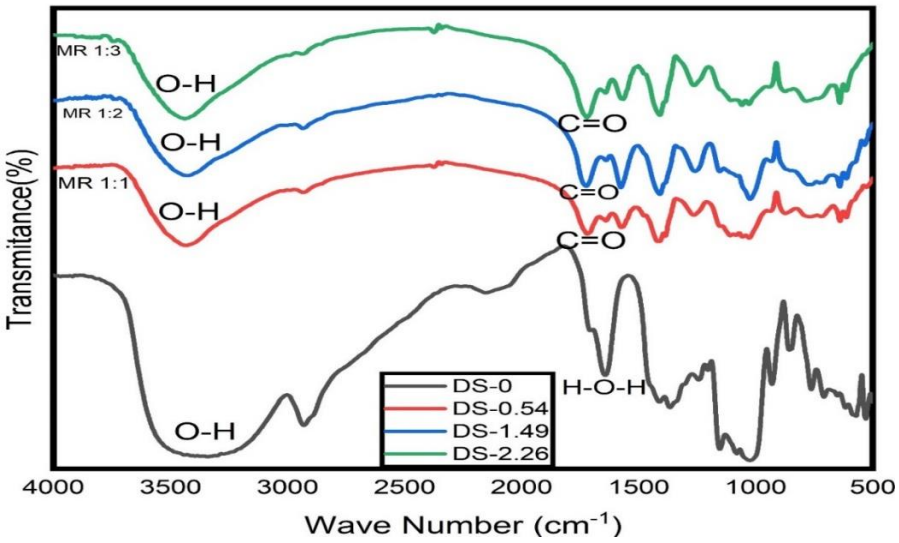


Figure 4. 15 Effect of mixing ratio on FTIR Spectra of native and modified starch

### 4.3.3. Effect of reaction time on DS

As shown in Table 4.9 DS is a function of the reaction times. For the reaction time from 60 to 240 min DS increased from 1.23 ± 0.2-2.39 ± 0.1. This increment of DS by prolonging the time of reaction was a direct consequence of the favorable effect of time on diffusion and adsorption of the acetic anhydride on the starch molecules [55, 57, 116]. However, the increment was nonlinear and characterized by an initial faster rate (DS from 1.23 ± 0.2 to 2.05 ± 0.09) followed by a slower rate (DS from 2.05 ± 0.09 to 2.39 ± 0.1). This can be described by the fact that as the reaction time prolonged , the acetic anhydride monomer was depleted, and also the reactive sites on the starch matrix decreased due to functional modification of the starch molecules[55]. Generally, acetic anhydride will contact the interior part of the starch matrix sufficiently as the reaction time increases. However, the DS decreases with the increasing of reaction time continuously, due to the completely consumption of acetic anhydride, and intensified degradation of starch will happen during the reaction process[102]. This result is also confirmed by FTIR analysis as shown in Fig.4.16 below

Table 4. 9 DS values measured by titration for different reaction time

| Temperature (℃ ) | Mixing ratio(w/w) | Reaction time(min) | Catalyst loading(w/w) | DS |
|---|---|---|---|---|
| 100 | 1:3 | 60 | 0.3 | 1.23 ± 0.2 |
| 100 | 1:3 | 120 | 0.3 | 2.05 ± 0.09 |
| 100 | 1:3 | 180 | 0.3 | 2.18 ± 0.05 |
| 100 | 1:3 | 240 | 0.3 | 2.39 ± 0.1 |

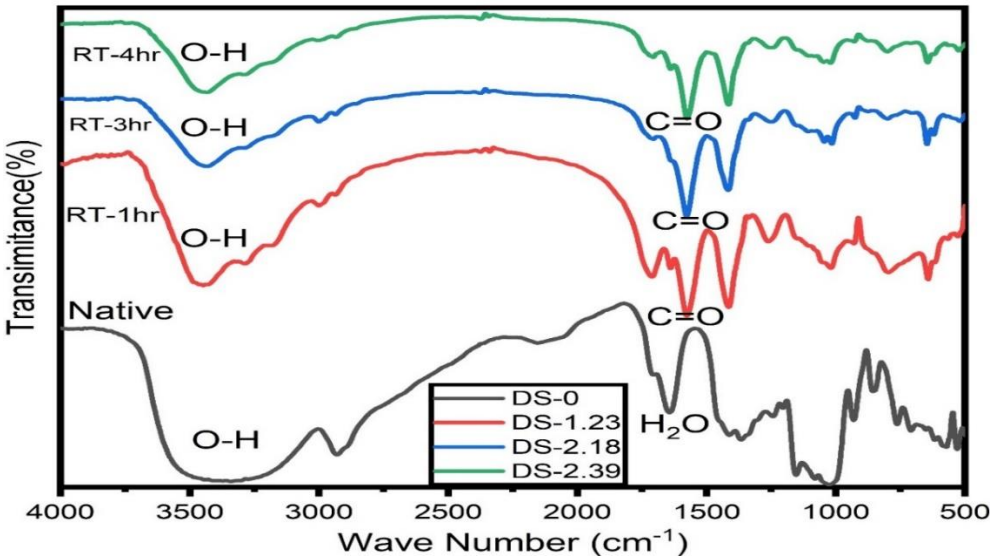


Figure 4. 16 Effect of reaction time on FTIR Spectra of native and modified starch

### 4.3.4. Effect of catalyst loading on DS

The NaOH was a catalyst that affected the reaction by swelling the starch matrix, thereby increasing the rate of diffusion of the acetic anhydride in the vicinity of starch matrix and by activating the hydroxyl groups(O-H) of starch to cause a nucleophilic attack on the anhydride moieties[55]. The effects of NaOH on DS was shown in Table 4.10, as amounts of NaOH increasing from 0.1-0.3 g/g of dry starch bases DS increased from 0.69 ± 0.4-1.9 ± 0.09 by keeping other reaction conditions constants. The DS decreased from 1.9 ± 0.09 to1.6 ± 0.12 when the NaOH loading increased from 0.3-0.4 g/g of dry starch bases. The increments were approximately nonlinear and characterized by an initial faster rate (DS from 0.69 ± 0.4 to 1.82 ± 0.09) followed by a slower rate (DS from 1.82 ± 0.09 to 1.9 ± 0.09). The increment of DS was associated with the abundant availability of acetic anhydride molecules around starch granules and free reactive sites on starch structure initially. As shown in Table 4.10 the loading of catalyst led to increasing levels of acetilazation, and starch acetates with DS as high as 1.9 ±

0.09 could be obtained. However, data showed that once a DS value of 1.9 ± 0.09 was achieved (catalyst load = 0.3 g/g starch), the use of a higher catalyst load did not result to a significant increase in the DS. At catalyst loading (0.4 g/g), decrement of DS was observed from 1.9 ± 0.09 to 1.6 ± 0.12, but still, the complete substitution (DS-3) of starch hydroxyls could not be reached. This may be due to a hindered access of acetic anhydride to a fraction of hydroxyl groups (O-H) which are not easily accessible for reaction. The accessibility of O-H on starch matrix is depend on its reactivity. It is known that the reactivity of the three free O-H groups of the anhydroglucose unit of starch decreases in the following order during starch modification: primary $C_6$ OH > secondary $C_2$ OH > secondary $C_3$ OH. Location of secondary hydroxyl groups within the interior surface of starch forming hydrogen bonds with the OH groups on the neighboring glucose units, makes these hydroxyl groups less accessible for esterification, justifying the incomplete acetylation even at high catalyst and acetic anhydride concentrations[101]. The result is also supported by FTIR analysis as shown in Fig.4.17 below

Table 4. 10 DS values measured by titration for different catalyst loading

| Temperature (℃ ) | Mixing ratio(w/w) | Reaction time (m) | Catalyst loading(g/g) | DS |
|---|---|---|---|---|
| 80 | 1:3 | 240 | 0.1 | 0.69 ± 0.4 |
| 85 | 1:3 | 240 | 0.2 | 1.82 ± 0.18 |
| 90 | 1:3 | 240 | 0.3 | 1.9 ± 0.09 |
| 100 | 1:3 | 240 | 0.4 | 1.6 ± 0.12 |

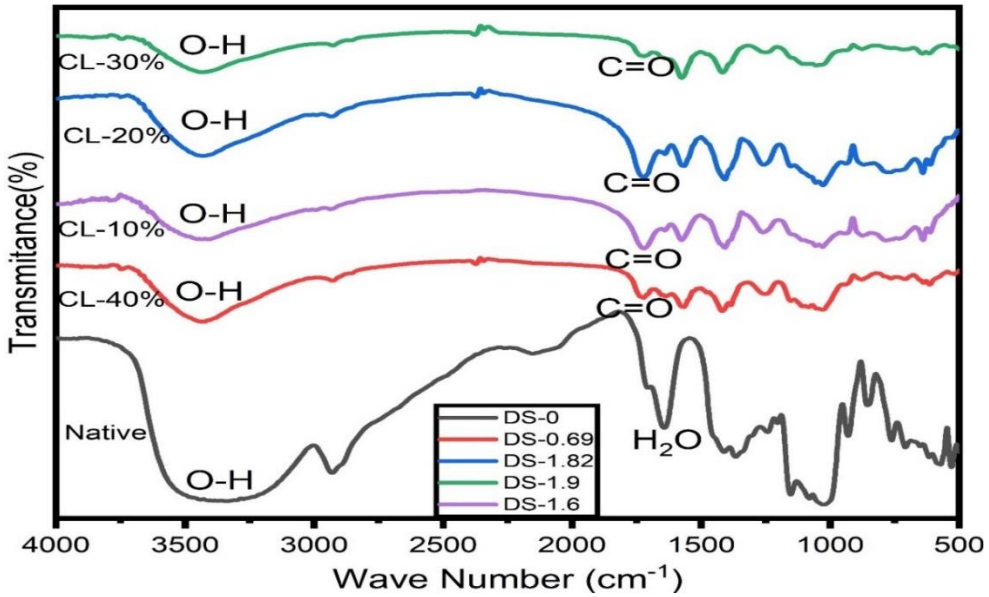


Figure 4. 17 Effect of catalyst loading on FTIR Spectra of native and modified starch

### 4.4. Lap shear strength analysis of anchote starch Adhesive

To determine the effect of the PVP and GA, on the lap shear strength of formulated adhesive, the chosen experimental approach was one parameter at a time. Following this experimental protocol the following results were observed as shown in Table 4.11 and Table 4.12. As shown in table 4.11 the lap shear strength increased significantly as the concentration of GA increased from 0% to 10%. When the concentration of GA was increased from 6% to 10%, the lap shear strength increased rapidly (24.4 to 44.59 Mpa), and from 0% to 6% the bonding strength shows a slowly increasing rate (17.42 to 24.4 MPa). Under this specific condition, the bonding strength of the formulated adhesive is 44.59 Mpa.

Table 4. 11 Effect of GA on the tensile strength of the Adhesive at 2 g PVP

| Modified Starch(g) | PVP (g) | GA (g) | BA (g) | Temp($^0$C) | Time (hr.) | Lap shears strength(Mpa) |
|---|---|---|---|---|---|---|
| 20 | 2 | 0 | 0.3 | 96 | 2.5 | 17.42 |
| 20 | 2 | 0.6 | 0.3 | 96 | 2.5 | 20.91 |
| 20 | 2 | 1.2 | 0.3 | 96 | 2.5 | 24.4 |
| 20 | 2 | 2 | 0.3 | 96 | 2.5 | 44.59 |

Also, as shown in Table 4.12, the lap shear strength increased significantly as the concentration of PVP increased from 0 to 2g. When the concentration of PVP was increased from 1.2 g to 2g, the lap shear strength increased rapidly (17.43 to 44.59 Mpa), and from 0 to 1.2g the lap shear strength shows a slowly increasing rate (5.53 to 17.43 MPa). Under this specific condition, the maximum lap strength of the formulated adhesive is 44.59 Mpa. The plot of stress versus strain for the maximum lap shear strength is shown in fig 4.18.

Table 4. 12 Effect of PVP on the tensile strength of the Adhesive at 2 g GA

| Modified Starch(g) | PVP (g) | GA (g) | BA (g) | Temp($^0$C) | Time (hr.) | Lap shear strength(Mpa) |
|---|---|---|---|---|---|---|
| 20 | 0 | 2 | 0.3 | 96 | 2.5 | 5.53 |
| 20 | 0.6 | 2 | 0.3 | 96 | 2.5 | 11.475 |
| 20 | 1.2 | 2 | 0.3 | 96 | 2.5 | 17.43 |
| 20 | 2 | 2 | 0.3 | 96 | 2.5 | 44.59 |

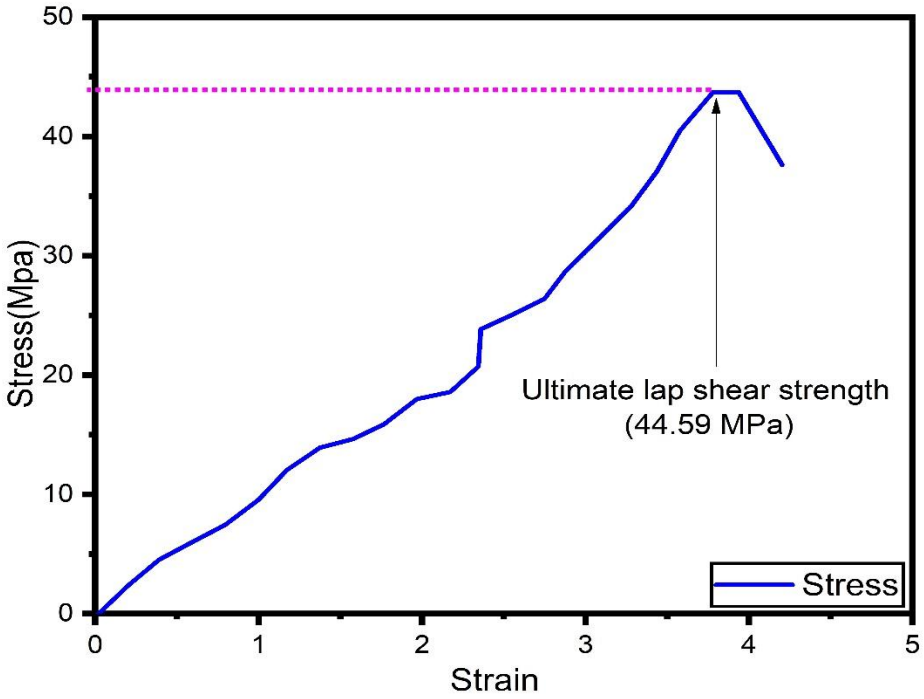


Figure 4. 18 Stress vs Strain diagram of ultimate lap shear strength

## 4.5. Effect of mixing parameters on Lap shear strength of the adhesive

### 4.5.1. Effect of Crosslinker boric acid (BA) on Lap shear strength

The lap shear strength of the adhesive at different boric acid (BA) concentrations by setting reaction temperature and mixing time constant has been investigated and the results are tabulated in Table 4.13. As the concentration of BA increased from 0 to 0.3 g, the increment of lap shear strength was observed from 12.6 to 44.5 Mpa, and from 0.3g to 0.6g a decrement in lap shear strength was observed from 44.5 to 33.6 Mpa. This may be due to the amount of BA in the solution increased, the possibility of cross-linking of free O-H in the solution increased and as a result lap shear strength increased in the range of 0-0.3g. The concentration of BA increases from 0.3 g to 0.6g, the lap shear strength decreases, this is due to the hindrance of crosslinking reaction between free O-H and BA [117]. During the crosslinking reaction BA can form a strong interaction between hydroxyl groups. The trivalent boron atom in boric acid has an empty p orbital that is very electrophilic, which causes it to rapidly react with various nucleophiles to form complexes, because the GA and starch are both rich in hydroxyl groups, boric acid can be expected to cross-link them and further improve the adhesion between the starch and GA blends [85]. The cross-linking mechanism of BA with OH group is given fig.4.19 the boric acid first forms the borate ion in the presence of water and further reacts with OH

groups which give the complex borate structure. The borate structure reacts with the nearby hydroxyl-containing chain which can be either of starch or GA/ PVP and finally structure was cross-linked.

Table 4. 13 Effect of Crosslinker (BA) on Lap shear strength

| Modified Starch(g) | PVP (g) | GA (g) | BA (g) | Temp($^0$C) | Time (hr.) | Lap shear strength(Mpa) |
|---|---|---|---|---|---|---|
| 20 | 2 | 2 | 0 | 96 | 2.5 | 12.695 |
| 20 | 2 | 2 | 0.3 | 96 | 2.5 | 44.59 |
| 20 | 2 | 2 | 0.6 | 96 | 2.5 | 33.69 |

### 4.5.2. Effect of mixing temperature on Lap shear strength

The result of mixing temperature effect on the lap shear strength of formulated adhesive, as BA concentration and mixing time was kept constant, was shown in Table 4.14 below. The mixing temperature increases from 50 $^0$C to 75 $^0$C, lap shear strength increased from 20.3MPa to 22.7 MPa. This may be due to the increased swelling power of starch as well as diffusion when the temperature increased from50 $^0$C to 75 $^0$C. The swelling of starch makes a favorable condition for the reaction of O-H with crosslink agents (BA). The tendency of swelling is directly proportionated with the temperature of the mixing [93]. As swelling power increases lap shear strength also shows increments. But temperature increases from 50 $^0$C to 75 $^0$C, lap shear strength increases from 20.3 Mpa to 22.7 Mpa, and temperature increases from 75 to 96 $^0$C, lap shear strength increases to 44.5 Mpa. These slow and fast increases of lap shear strength may be highly associated with the swelling tendency of starch as a result of mixing temperature.

Table 4. 14 Effect of mixing temperature on Lab shear strength

| Modified Starch(g) | PVP (g) | GA (g) | BA (g) | Temp($^0$C) | Time (hr.) | Tensile strength(Mpa) |
|---|---|---|---|---|---|---|
| 20 | 2 | 2 | 0.3 | 50 | 2.5 | 20.3 |
| 20 | 2 | 2 | 0.3 | 75 | 2.5 | 22.7 |
| 20 | 2 | 2 | 0.3 | 96 | 2.5 | 44.5 |

### 4.5.3. Effect of mixing time on Lap shear strength

AS shown in table 4.15 the effect of mixing time on the lap shear strength of adhesive at constant BA concentration (0.3 g) and mixing temperature (96 $^0$C). As mixing time increases from 1hr. to 2.5 hr., lap shear strength increased significantly from 21.2MPa to 44.5 MPa. Beyond 2.5 hr., lap shear strength decreases to 43.3 Mpa at a time of 4 hr. This showed us, no significant difference in lap shear strength was observed as mixing time increases. This result shows that the use of excess mixing time on lap shear strength has no effect rather than wasting energy. The result of the lap shear strengths of the adhesive as a function of mixing time indicate that effective mixing of, PVP, GA, and BA with modified Starch was achieved within 2.5 hr. Therefore, 2.5 hr. was an appropriate mixing time for this specific condition.

Table 4. 15 Effect of mixing Time on Lab shear strength

| Modified Starch(g) | PVP (g) | GA (g) | BA (g) | Temp($^0$C) | Time (hr.) | Tensile strength(Mpa) |
|---|---|---|---|---|---|---|
| 20 | 2 | 2 | 0.3 | 96 | 1 | 21.2 |
| 20 | 2 | 2 | 0.3 | 96 | 2.5 | 44.5 |
| 20 | 2 | 2 | 0.3 | 96 | 4 | 43.3 |

## 4.6. Performance Improvement of starch-based adhesive

### 4.6.1. Improvement of Lap shear strength

According to the Table 4.16, formulated adhesive from native anchote starch has too weak adhesive properties to adhere wood specimens with each other. These bonded specimens were simply detached by pulling by hand or applying very small force. This weak binding of native anchote starch was the result of forming a hydrogen bond with O-H groups of starch during mixing processes. To improve this drawback of native anchote starch, esterification modification had done and brought an improvement of lab shear strength to 2.13 Mpa. However, esterification modification native anchote brought significant improvement in adhesive nature, it can't full fill the minimum criteria of the adhesive which was ≥ 2.32 Mpa. To meet the minimum requirements of adhesive, GA and PVP are incorporated with modified anchote starch as adhesive enhancers and BA as Crosslinker agent. The result of adhesive nature enhancers PVP/ GA and Crosslinker BA were tabulated below in Table 4.16. These results confirm that the adhesive nature of modified anchote starch was significantly improved to 44.5 Mpa by

adding 2g GA, 2g PVP, and 0.3g BA. This value was nearly comparable with commercially available polyvinyl acetate (PVAc) is 43.13 Mpa.

Table 4. 16 Lap shear strength improvement

| Mixing components | Mixing conditions | | | Lap shear strength (Mpa) |
|---|---|---|---|---|
| | Temp ($^0$C) | Time (hr.) | RPM | |
| Before modification (native starch paste) | 96 | 2.5 | 170 | Bonded Specimen simply detached by pulling with the hand |
| Modified starch | 96 | 2.5 | 170 | 2.13 Mpa |
| Modified starch + 0.3g BA | 96 | 2.5 | 170 | 3.13 Mpa |
| Modified starch +2g (PVP) | 96 | 2.5 | 170 | 17.42 Mpa |
| Modified starch +2g, GA | 96 | 2.5 | 170 | 5.13 Mpa |
| Modified starch +0.3g BA+2g PVP+2g GA | 96 | 2.5 | 170 | 44.59 Mpa |
| Commercial available PVAc | | | | 43.13 Mpa |

### 4.6.2. Improvement of Water Resistance

Anchote starch modification by acetilazation was used to improve the water-resisting capacity of adhesive as shown in table 4.17. When compared to the native anchote starch-based adhesive of 0.3 g BA, 2 g GA, and 2 g PVP with modified anchote starch adhesive of 0.3 g of BA, 2 g GA, and 2 g of PVP, the modified anchote starch adhesive increased the hydrophobicity characteristics by 72.1% in the wet state. This implies that starch modification significantly enhance the water resisting property of adhesive by reducing the O-H group of starch by replacing it with hydrophobic acetyl groups. This result suggest that, the functionally modified

anchote starch can be used as potential raw material to formulate environmentally friendly starch-based adhesive with good performance.

Table 4. 17 Improvement of water resistance

| Mixing components | Tensile strength Before soaking in water | After soaking in water for 24.hr at room temp | Hydrophilicity (%) |
|---|---|---|---|
| Native starch (20g) +0.3 g BA+ 2 g PVP+ 2 g GA | 33.69 Mpa | Bonded sample easily detached by pulling by hand | 100 |
| Modified starch (20g) + 0.3 g BA+2 g PVP+ 2g GA | 44.59 Mpa | 25.45 Mpa | 27.3 |

## 4.7. Characterization of the modified starch-based adhesives.

From the lab shear strength analysis of section 4.4, a Sample with a mixture of (modified starch + 0.3 g BA + 2 g GA and 2 g PVP) was selected for characterization as it gave the maximum lap shear strength of 44.53 MPa**.**

### 4.7.1. Characterization of Adhesive by FTIR analysis

Intermolecular interactions of modified anchote starch, BA, GA, and PVP were proved by comparing spectra of them with spectra of modified starch +0.3 g BA + 2 g GA +2 g PVP as shown in fig 4.20. The clear changes in the molecular structure of modified starch, GA, and PVP were noticed from FTIR. Fig.4.20 exhibit the FTIR spectra of modified anchote starch, GA ,PVP, and modified anchote starch + 0.3 g BA + 2 g GA + 2 g PVP prepared by mixing. The FTIR spectra of GA showed the broad absorption band at 3404 $cm^{-1}$ due to stretching vibration of the O-H group, N-H group, and glycosidic ring [81] as shown in zone 1 of Fig 4.20. The same broadband vibrations of O-H were found in modified starch +0.3 g BA + 2 g GA +2 g PVP adhesive matrix. The peak also shifted toward a higher wavenumber and was found at 3448 $cm^{-1}$ and the intensity of O-H decreases. It suggests that the crosslinking happened at the O-H group. A peak at 1606 $cm^{-1}$ in GA attributed to the COO asymmetric stretching which was merged and shifting of peaks was observed in modified starch +0.3 g BA + 2 g GA +2 g PVP as shown in zone 2. It confirmed that a chemical reaction was taking place during mixing. As shown in zone 3, a broad vibration was observed at 1057 $cm^{-1}$ in GA which is the fingerprint

spectra of carbohydrates present in the sample [81]. Here also, the broad vibrational band disappeared and merged with modified starch +0.3 g BA + 2 g GA +2 g PVP. This also confirmed that chemical reactions happened during mixing.

The FTIR spectra of PVP showed the broad absorption band at 3456 $cm^{-1}$ due to stretching vibration of the O-H group[118] as shown in zone 1 of fig 4.20. The same broadband vibrations of O-H were found in modified starch +0.3 g BA + 2 g GA + 2 g PVP sample. But, its transmittance intensity was much smaller than that of PVP. The peak also shifted toward a lower wavenumber and was found at 3448 $cm^{-1}$ and the intensity of O-H decreases. It suggests that the chemical reaction happened at the free site of the O-H group. A peak at 1665 $cm^{-1}$ in PVP attributed to the C=O stretching vibration which was merged and shifting of peaks was observed in modified starch +0.3 g BA + 2 g GA +2 g PVP [118] as shown in zone 2. It suggested that a chemical mixing was occurred during mixing processes. As shown in zone 3, the absorption bands at 1493 $cm^{-1}$ were assigned to the vibration of the pyrrolidone (PVP) ring. Here also, the vibrational of PVP ring not disappeared but it merged with modified starch +0.3 g BA + 2 g GA + 2 g PVP by a slight shifting of peaks. This also confirmed that chemical reactions happened during mixing.

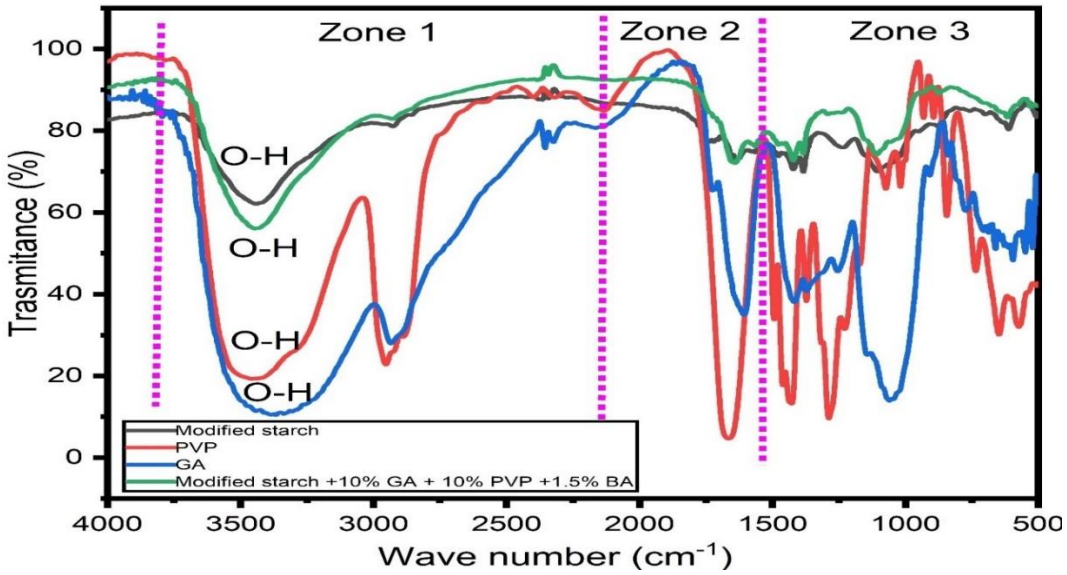

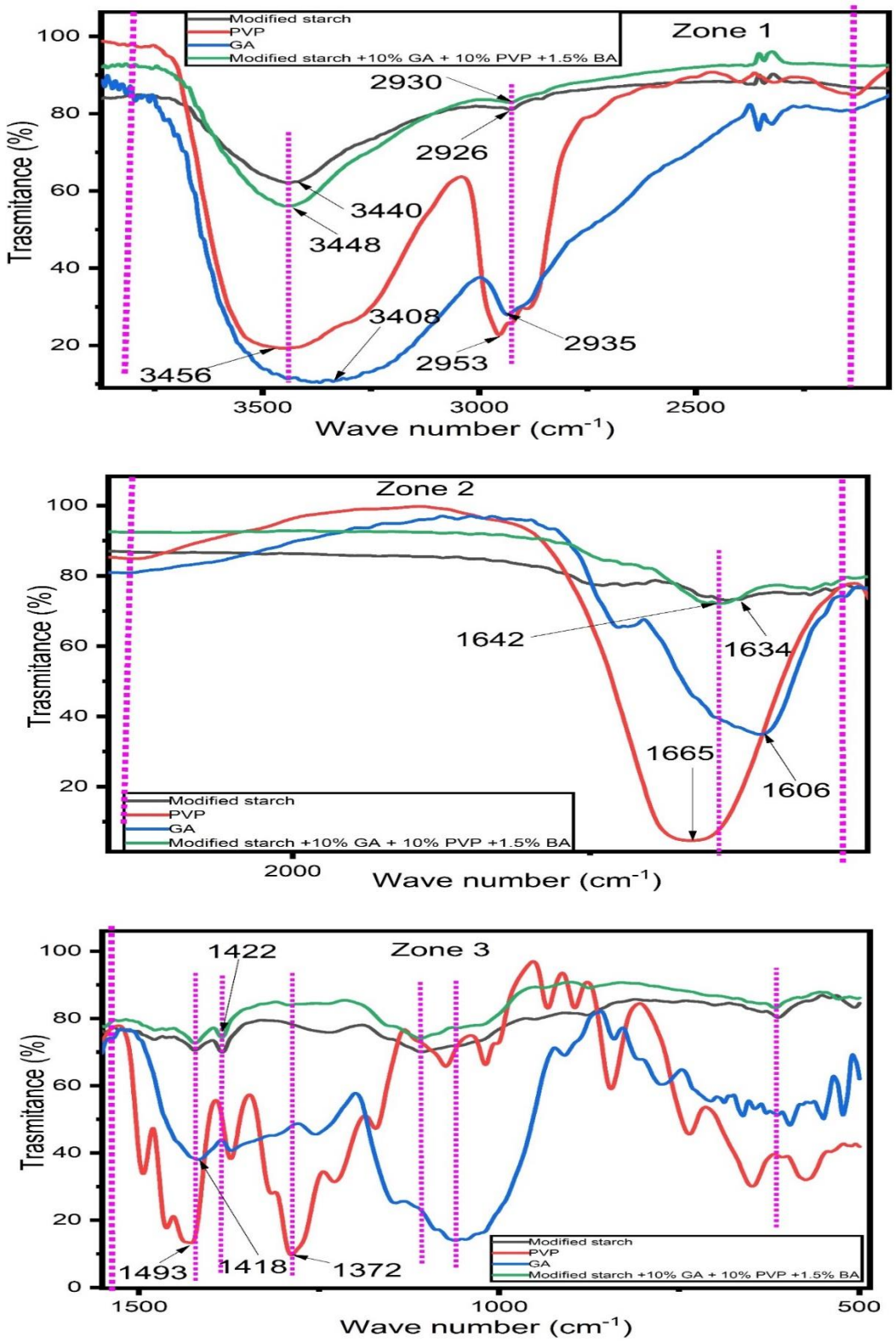


Figure 4. 19 FTIR spectra of modified starch, GA, PVP, and modified starch +0.3 g BA +2 g GA+ 2 g PVP

### 4.7.2. Characterization of Adhesive by thermogravimetric (TGA) analysis

TGA has been used extensively in the study of polymeric structures. This analytical technique is used to determine materials' thermal stability and their fraction of volatile components by observing the weight loss of the sample in a chosen atmosphere as a function of temperature. Fig.4.21, shows the TGA experimental results of modified starch, GA, PVP, and blend of modified starch with 0.3 g BA, 2 g GA, and 2 g of PVP. The matrix was measured in the temperature range from 30 $^0$C to 700 $^0$C with a constant rate of 20 $^0$C/min under a nitrogen atmosphere. In Figure 4.21, TGA and DTG show that the weight loss of the samples decreases as the temperature increases, and all samples experienced weight loss in three major stages. The first stage involves the evaporation of absorbed water at a temperature range of 60–120 $^0$C [46]. The second step exhibits the decomposition of side chains and the third stage correspond to the decomposition and the dehydration of main polymer chains [119]. Water is formed by inter-and intramolecular condensation of hydroxyl groups. It is the main product of decomposition below about 300 $^0$C. When the temperature is heating up to 700 $^0$C, this eventually results in carbonization, and the formation of ash and $CO_2$ is released [46]. As shown in Table 4.18, it can be seen that the major weight loss is occurred at about 80-90 Wt% in the range of 200-500ºC for all samples which correspond to the structural decomposition. A typical weight loss occurred at about 100 $^0$C due to evaporation and the mass loss from 100ºC to the onset decomposition temperature is related to water and other volatile components [119].

The onset temperatures of the weight loss were 199 $^0$C,262 $^0$C ,410 $^0$C and 197 $^0$C for modified starch ,GA ,PVP and modified starch mixed with 0.3 g BA, 2 g GA, and 2 g PVP, respectively. As observed on the DTG curve in Fig 4.21 (B), the modified starch mixed with 0.3 g BA, 2g GA, 2 g PVP had a lower maximum temperature ($T_{max}$) of 240 $^0$C as compared to the other components as shown in Table 4.18. This indicated that the modified starch mixed with 0.3 g BA, 2 g GA, and 2 g PVP was less thermally stable. This less thermal stability associated with introduction of BA into the matrix, which speed up catalyzing effect as temperature increases. The weight loss of modified starch mixed with 0.3 g BA, 2 g GA, and 2 g PVP at $T_{90}$ showed an increase in mass loss relative to modified starch and a decrease relative to GA and PVP with the addition of the GA and PVP. The thermal decomposition of modified starch mixed with 0.3 g BA, 2 g GA, and 2 g PVP shifted slightly toward lower temperature compared to GA and PVP and slightly shifted to higher temperature compared to modified starch. This can be concluded

that modified starch blend with 0.3 g BA, 0.3 g GA, and 0.3 g PVP suppresses the thermal stability of GA and PVP and this confirms that there is a molecular interaction or chemical reaction between modified starch, GA, and PVP [119].

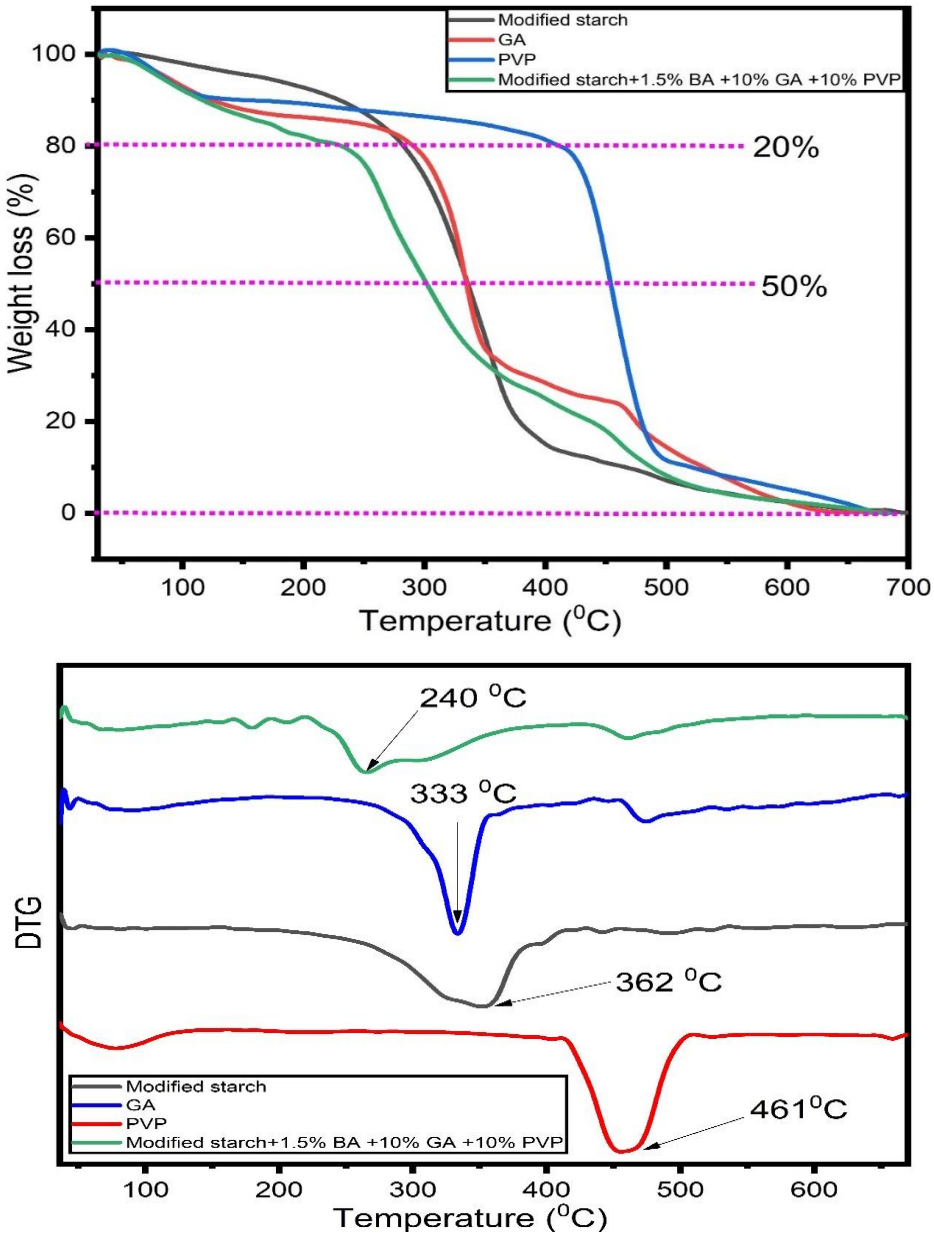


Figure 4. 20 TGA and DTG curves for the modified starch, GA, PVP and modified starch + 0.3 g BA +2 g GA + 2 g PVP

Table 4. 18 Thermal characteristics of modified starch, GA, PVP and modified starch + 0.3 g BA +2 g GA + 2 g PVP

| Sample | $T_{20\%}$ ($^0$C) | $T_{50\%}$ ($^0$C) | $T_{90\%}$ ($^0$C) | $T_{max}$ ($^0$C) |
|---|---|---|---|---|
| Modified starch | 281 | 335 | 459 | 362 |
| GA | 290 | 335 | 535 | 333 |
| PVP | 412 | 454 | 515 | 461 |
| Modified starch + 0.3 g BA + 2 g GA+2 g PVP | 225 | 302 | 487 | 240 |

# CHAPTER FIVE

# 5. CONCLUSION AND RECOMMENDATION

## 5.1. Conclusion

This research focuses on extracting and structural modification of anchote (*Coccinia abyssinica* (Lam.) Cogn.) starch for bio-based adhesive applications. Starch was extracted and characterized from anchote (*Coccinia abyssinica* (Lam.) root from Wollega, Ethiopia. The SEM analysis confirmed that most of its granules were dome-shaped with polygonal or irregular shape on geometry and the size of the granules varied from 2.21 to 19.99 μm. It gave B-type starch by showing a strong peak at $17^{0}$ of $2\theta$ when analyzed by x-ray powder diffraction (XRD). Its higher gelatinization temperature (79.9 $^{0}$C) in DSC analysis implies that the higher crystallinity is there in anchote starch. FTIR analysis observed the broad bands at (3010-3600) $cm^{-1}$ for native anchote starches indicate the stretching vibrations of O-H groups. The highest decomposition occurred in the range of 128–321 ℃, and the temperature of maximum weight loss rate ($T_{max}$) of native starch occurred at 321℃ when analyzes by TGA/DTG. These properties of anchote starch conclude it as a potential candidate for thermoplastic starch products.

Anchote starch acetates with various degrees of substitution (DS) were prepared by reaction of native starch with acetic anhydride using aqueous sodium hydroxide (NaOH) as a catalyst. The degree of substation (DS) increased with increasing temperatures, reaction times, and increasing mixing ratios of acetic anhydride to starch. Increasing the amount of catalyst NaOH up to 30% increases DS and decreases DS beyond 30% due to the occurrence of steric hindrance. Selected starch acetates with DS (0.54, 1.49, 2.26, and 3) were investigated for structural properties after modification. Structural modification of starch resulted in substantial changes in the physicochemical properties of the native starch. The FT-IR spectra confirm that the peak of the carbonyl group (C=O) appeared at 1,739 $cm^{-1}$ for DS-3 due to the introduction of the acetyl group on native starch. X-ray diffraction (XRD) approved that the crystal structure of native starch was disappeared and gradually converted to an amorphous structure for DS-3. The scanning electron microscopy (SEM) images indicated a substantial variation in starch

morphology and the smooth surface of the starch granules converted rough surface as DS increases. The thermal stability of acetylated starch depends on the degree of substitution (DS) according to the experimental results of DSC and TGA/DTG. The DSC results revealed that acetylated anchote starches had decreasing values of To, Tp, Tc, and ΔHgel and, the higher gelatinization temperature range (Tc-To) as DS increases. According to TGA/DTG results, the thermal stability of acetylated starch with high DS (DS-3) which was 362 ℃ is much better than that of the native starch at 321 ℃. This increment of thermal stability of starch acetates is associated with the decreasing of the hydroxyl (O-H) groups of native starch at 3000-3600 $cm^{-1}$ by replacing them with the acetyl groups.

Modified starch-based adhesive with various lap shear strength was prepared by reaction of modified starch with GA, and PVP using Boric acid (BA) as a Crosslinker. The lap shear strength increased with increasing PVP, GA, mixing temperature, and increasing concentration of BA to 0.3 g. The concentration of BA increases from 0.3 g to 0.6 g, the lap shear strength decreases, this is due to the hindrance of crosslinking reaction between free OH and BA. Increasing the mixing time up to 2.5 hr. increases lap shear strength and no significant difference in lap shear strength was observed as mixing time increases to 4 hr. This result shows that the use of excess mixing time on lap shear strength has no effect rather than wasting energy.

Intermolecular interactions of modified anchote starch, BA, GA, and PVP were proved by (FTIR) analysis by comparing spectra of them with spectra of adhesive prepared by modified starch,0.3 g BA, 2 g GA, and 2 g PVP. The clear changes in the molecular structure of modified starch, GA, and PVP were noticed from FITR analysis. The changes with the shifting of peaks confirm the occurrence of intermolecular interaction or chemical reactions during the mixing process. Also, TGA analysis confirmed the occurrence of molecular interaction or chemical reaction between modified starch, GA, and PVP by the thermal decomposition. Modified starch mixed with 0.3 g BA, 2 g GA, and 2 g PVP shifted slightly toward lower temperature compared to GA and PVP and slightly shifted to higher temperature compared to modified starch. This can be concluded that modified starch blend with 0.3 g BA, 2 g GA, and 2 g PVP suppresses the thermal stability of GA and PVP and this confirms that there is a molecular interaction or chemical reaction between modified starch, GA, and PVP.

## 5.2. Recommendation

The extraction and structural modification of anchote (*Coccinia abyssinica* (Lam.) Cogn.) starch for adhesive application was studied. The modified starch has a promising property with the required adhesive characterization such as lap shear strength and water resistivity. Due to financial and technical instrument constraints, the scope of thesis work was limited at this level. Base on the present study, some recommendations can be made for future work.

- Further work on modified starch-based adhesive preparation was recommended by optimizing parameters and detailed study on properties of adhesive.
- Gum arabic (GA) and, Polyvinylpyrrolidone (PVP) modification and characterization was recommended to enhance water resistance and tensile strength
- NMR analysis of modified starch and prepared adhesive were recommended to understand the intermolecular interaction that occurred during the reaction.
- Further studies were needed on Ethiopian indigenous anchote (*Coccinia abyssinica* (Lam.) Cogn.) starch for different applications.
- This thesis work recommended that anchote starch was a potential candidate for thermoplastic starch products.

# REFERENCES


1. Bandara, N.P., Nanoengineered And Biomimetic Protein-Derived Adhesives With Improved Adhesion Strength And Water Resistance. 2017.
2. Ferdosian, F., Et Al., Bio-Based Adhesives And Evaluation For Wood Composites Application. Polymers, 2017. 9(2): P. 70.
3. Alawode, A.O., Et Al., Properties And Characteristics Of Novel Formaldehyde-Free Wood Adhesives Prepared From Irvingia Gabonensis And Irvingia Wombolu Seed Kernel Extracts. International Journal Of Adhesion And Adhesives, 2019. 95: P. 102423.
4. Chen, M., Et Al., Soybean Meal-Based Wood Adhesive Enhanced By Phenol Hydroxymethylated Tannin Oligomer For Exterior Use. Polymers, 2020. 12(4): P. 758.
5. Antov, P., V. Savov, And N. Neykov, Sustainable Bio-Based Adhesives For Eco-Friendly Wood Composites. A Review. Wood Research, 2020. 65(1): P. 51-62.
6. Gadhave, R.V., P.A. Mahanwar, And P.T. Gadekar, Starch-Based Adhesives For Wood/Wood Composite Bonding. 2017.
7. Qi, G., Modified Soy Protein Based Adhesives And Their Physicochemical Properties. 2011.
8. Lin, Q., Et Al., Development And Mechanism Characterization Of High Performance Soy-Based Bio-Adhesives. International Journal Of Adhesion And Adhesives, 2012. 34: P. 11-16.
9. Lambuth, A.L., The Applications Of Wood Adhesives Have Risen Tremendously. 1989, ACS Publications.
10. Sandberg, D., Additives In Wood Products—Today And Future Development, In Environmental Impacts Of Traditional And Innovative Forest-Based Bioproducts. 2016, Springer. P. 105-172.
11. Addis, C.C., R.S. Koh, And M.B. Gordon, Preparation And Characterization Of A Bio-Based Polymeric Wood Adhesive Derived From Linseed Oil. International Journal Of Adhesion And Adhesives, 2020. 102: P. 102655.
12. Wang, Z., Et Al., Improvement Of The Bonding Properties Of Cassava Starch-Based Wood Adhesives By Using Different Types Of Acrylic Ester. International Journal Of Biological Macromolecules, 2019. 126: P. 603-611.
13. Xing, J., Et Al., Development And Characterization Of A New Bio-Adhesive For Wood Using Cassava Starch And Bio-Oil. International Journal Of Adhesion And Adhesives, 2018. 87: P. 91-97.
14. Wang, Z., Et Al., Bonding Strength And Water Resistance Of Starch-Based Wood Adhesive Improved By Silica Nanoparticles. Carbohydrate Polymers, 2011. 86(1): P. 72-76.

15. Chen, L., Et Al., Effects Of Nano-Tio2 On Bonding Performance, Structure Stability And Film-Forming Properties Of Starch-G-Vac Based Wood Adhesive. Carbohydr Polym, 2018. 200: P. 477-486.
16. Bhattacharya, A. And B.N. Misra, Grafting: A Versatile Means To Modify Polymers: Techniques, Factors And Applications. Progress In Polymer Science, 2004. 29(8): P. 767-814.
17. Chen, L., Et Al., Sodium Dodecyl Sulfate Improves The Properties Of Bio-Based Wood Adhesive Derived From Micronized Starch: Microstructure And Rheological Behaviors. Int J Biol Macromol, 2019. 140: P. 1026-1036.
18. Liu, Y. And K. Li, Development And Characterization Of Adhesives From Soy Protein For Bonding Wood. International Journal Of Adhesion And Adhesives, 2007. 27(1): P. 59-67.
19. Ogunsona, E., E. Ojogbo, And T. Mekonnen, Advanced Material Applications Of Starch And Its Derivatives. European Polymer Journal, 2018. 108: P. 570-581.
20. Sun, Y., Et Al., Physicochemical Properties Of Starch Adhesives Enhanced By Esterification Modification With Dodecenyl Succinic Anhydride. Int J Biol Macromol, 2018. 112: P. 1257-1263.
21. Yambo, Y. And T. Feyissa, Micropropagation Of Anchote [Coccinia Abyssinica (Lam.) Cogn.]: High Calcium Content Tuber Crop Of Ethiopia. African Journal Of Agricultural Research, 2013. 8(46): P. 5915-5922.
22. Hassen Yassin, A.M., D. Fekadu, And S. Hussen, Effect Of Flower Bud Removal On Growth And Yield Of Anchote Root (Coccinia Abyssinica (Lam.) Cogn.) Accessions At Bishoftu. 2013.
23. Abera, G., Et Al., Comparison Of Physicochemical Properties Of Indigenous Ethiopian Tuber Crop (Coccinia Abyssinica) Starch With Commercially Available Potato And Wheat Starches. International Journal Of Biological Macromolecules, 2019. 140: P. 43-48.
24. Fekadu, H., F. Beyene, And G. Desse, Effect Of Traditional Processing Methods On Nutritional Composition And Anti-Nutritional Factors Of Anchote (Coccinia Abyssinica (Lam.) Cogn.) Tubers Grown In Western Ethiopia. J Food Process Technol, 2013. 4(7): P. 249.
25. Fekadu, H., Nutritional Composition, Antinutritional Factors And Effect Of Boiling On Nutritional Composition Of Anchote (Coccinia Abyssinica) Tubers. Food Science And Quality Management, 2014. 26: P. 25-38.
26. Fekadu, H., F. Beyene, And G. Haki, Evaluation Of Bioavailability And Sensory Preference Of Processed Anchote (Coccinia Abyssinica) Tubers In Eastern Wollega, Ethiopia. J. Food Nutr. Sci, 2014. 2: P. 1-12.
27. Bekele, A., T. Feyissa, And K. Tesfaye, Genetic Diversity Of Anchote (Coccinia Abyssinica (Lam.) Cogn.) From Ethiopia As Revealed By ISSR Markers. Genetic Resources And Crop Evolution, 2014. 61(3): P. 707-719.

28. Kahia, J., P. Njenga, And M. Kirika, Improved Micropropagation Of Plantlets From Nodal Explants Of Anchote (Coccinia Abyssinica)—A Calcium-And Protein-Rich Tuber. Hortscience, 2016. 51(7): P. 905-909.
29. Mekbib, Y. And T. Deressa, Exploration And Collection Of Root And Tuber Crops In East Wollega And Ilu Ababora Zones: Rescuing Declining Genetic Resources. 2016.
30. Abera, G. And D. Haile, Yield And Nutrient Concentration Of Anchote [Cocciniaabyssinica (Lam.) Cogn.] Affected By Harvesting Dates And In-Situ Storage. African Journal Of Crop Science, 2015. 3(5): P. 156-161.
31. Desalegn, B.B., F.T. Tadesse, And D. Haile, Physical And Proximate Characterization Of Anchote (Coccinia Abyssinica) Accessions Grown Under Hawassa And Wondo Genet Conditions, Southern Ethiopia. Food Science And Quality Management, 2015. 42: P. 62-74.
32. Ayalew, Y., Nutritional And Phytochemical Evaluation Of Anchote (Cocciniaabyssinica)(Lam.)(Cogn.) Accessions To Promote Its Contribution For Food Security And Medicinal Use. 2016.
33. Parmar, A., Et Al., Nutritional Comparison Of White And Red Coccinia Abyssinica (Lam.) Cong. Accessions: An Under-Utilised Edible Tuber Of The Ethiopian Highlands. Foods, 2017. 6(8): P. 71.
34. Mosissa, A., Y. Bekele, And T. Berhanu, Food And Nutrition Security Potential Of Anchote (Cocciniaabyssinica); A Tuberous Crop Indigenous To Ethiopia: A Review. International Journal Of Food Engineering And Technology, 2019. 7(2): P. 34-38.
35. Fufa, T.W., Genetic Variability And Association In Yield And Yield Related Traits In Anchote [Coccinia Abyssinica (Lam.) Cogn.]. 2012.
36. Ayana, N.G., Agricultural Science Research Journal ISSN.
37. Feyissa, Y.Y.A.T., Micropropagation Of Anchote [Coccinia Abyssinica (Lam.) Cogn.]: High Calcium Content Tuber Crop Of Ethiopia. African Journal Of Agricultural Research, 2013.
38. Duresso, M.E., Study On Ethnobotany And Phenotypic Diversity In Anchote (Coccinia Abyssinica (Lam.) Cogn.) Landraces In Western Ethiopia.
39. Feyissa, T., Coccinia Abyssinica (Lam.) Cogn.(Anchote) Biology, Productivity, And Prospects Of Genetic Improvement Using Biotechnological Tools. Journal Of Horticultural Research, 2020. 1(Ahead-Of-Print).
40. Mitiku, D.H. And A.F. Roro, Nutritional Potential And Antnutritional Factors Of Plectranthus Edulis, Cocciniaabyssinica And Dioscoreaabyssinica Tubers: A Review. Science Research, 2020. 8(1): P. 7.
41. Abate, S., F. Mekbib, And E. Gebre, In Vitro Somatic Embryogenesis And Plantlet Regeneration In Anchote [Coccinia Abyssinica (Lam.) Cong.]. Plant Physiology Reports, 2019. 24(3): P. 351-358.
42. Fekadu, D., Phenotypic And Nutritional Characterization Of. 2011.

43. Habtamu Fekadu, E.A., Evaluation Of Bioavailability And Sensory Preference Of Processed Anchote (Coccinia Abyssinica) Tubers In Eastern Wollega, Ethiopia Journal Of Food And Nutrition Sciences, 2013.
44. Shebabaw, H., Effect Of Processing On Physicochemical And Antinutritional Factors Of "Anchote"(Coccinia Abyssinica) And Development Of Value Added Biscuit. 2013.
45. Cynthia Fabian A, A.A.B., Suryadi Ismadji B, Yi-Hsu Ju A,*, Solation And Characterization Of Starch From Defatted Rice Bran. Journal Of The Taiwan Institute Of Chemical Engineers, 2011.
46. Lamaming, J., Et Al., Characterization Of Rubberwood Particleboard Made Using Carboxymethyl Starch Mixed With Polyvinyl Alcohol As Adhesive. Composites Part B: Engineering, 2020. 183: P. 107731.
47. Idrees Ahmed Wani, D.S.S., Afshan Mumtaz Hamdani, Adil Gani, Naseer Ahmad Bhat And Asima Shah, Isolation, Composition, And Physicochemical Properties Of Starch From Legumes: A Review. Starch/Stärke 2016.
48. Lemos, P.V.F., Et Al., Structural And Thermal Investigations Of Starch Polymers As Matrices For Retention Of Rhynchophorol Aggregation Pheromone. Journal Of Thermal Analysis And Calorimetry, 2020: P. 1-14.
49. Fazal Haqa, H.Y., ∗∗, Li Wanga,∗, Lisong Tengb, Muhammad Haroona, Rizwan Ullah Khana, And B.-U.-A. Sahid Mehmooda, Raja Summe Ullaha, Amin Khana, Ahsan Nazira, Advances In Chemical Modifications Of Starches And Their Applications. 2019.
50. Mo, O., Tacca Starch: A Review Of Its Production, Physicochemical Properties,Modification And Industrial Uses. African Journal Of Food, Agricultural ,Nuturatinal And Development, 2013.
51. Imre, B. And F. Vilaplana, Organocatalytic Esterification Of Corn Starches Towards Enhanced Thermal Stability And Moisture Resistance. Green Chemistry, 2020. 22(15): P. 5017-5031.
52. Zhang, Y., Et Al., Preparation And Properties Of A Starch-Based Wood Adhesive With High Bonding Strength And Water Resistance. Carbohydrate Polymers, 2015. 115: P. 32-37.
53. Chen, L., Et Al., Investigating The Structure And Self-Assembly Behavior Of Starch-G-Vac In Starch-Based Adhesive By Combining NMR Analysis And Multi-Scale Simulation. Carbohydrate Polymers, 2020. 246: P. 116655.
54. Din, Z.U., Et Al., Starch: An Undisputed Potential Candidate And Sustainable Resource For The Development Of Wood Adhesive. Starch-Stärke, 2020. 72(3-4): P. 1900276.
55. Xu, Y., V. Miladinov, And M.A. Hanna, Synthesis And Characterization Of Starch Acetates With High Substitution. Cereal Chemistry, 2004. 81(6): P. 735-740.
56. Xu, J., T.D. Andrews, And Y.C. Shi, Recent Advances In The Preparation And Characterization Of Intermediately To Highly Esterified And Etherified Starches: A Review. Starch-Stärke, 2020. 72(3-4): P. 1900238.

57. Cuenca, P., S. Ferrero, And O. Albani, Preparation And Characterization Of Cassava Starch Acetate With High Substitution Degree. Food Hydrocolloids, 2020. 100: P. 105430.
58. Diop, C.I.K., Et Al., Effects Of Acetic Acid/Acetic Anhydride Ratios On The Properties Of Corn Starch Acetates. Food Chemistry, 2011. 126(4): P. 1662-1669.
59. Trela, V.D., A.L. Ramallo, And O.A. Albani, Synthesis And Characterization Of Acetylated Cassava Starch With Different Degrees Of Substitution. Brazilian Archives Of Biology And Technology, 2020. 63.
60. Dumancela, K., E. Mayorga, And J. Santamaría-Aguirre, Acetylation Of Starch Extracted From Rejected Fruits Of Musa× Paradisiaca L. To Obtain A Pharmaceutical Disintegrant. Pharmacology & Pharmacy, 2020. 11(06): P. 118.
61. Gu, Y., Et Al., Preparation, Characterization And Properties Of Starch-Based Adhesive For Wood-Based Panels. International Journal Of Biological Macromolecules, 2019. 134: P. 247-254.
62. Wang, Z., Et Al., Preparation, Characterization And Properties Of Starch-Based Wood Adhesive. Carbohydrate Polymers, 2012. 88(2): P. 699-706.
63. Zhang, Y., Et Al., Synthesis Of Grafting Itaconic Acid To Starch-Based Wood Adhesive For Curing At Room Temperature. Journal Of Polymers And The Environment, 2020: P. 1-9.
64. Da Silva, L.F.M., A. Öchsner, And R.D. Adams, Handbook Of Adhesion Technology. 2011: Springer Science & Business Media.
65. Vick, C.B., Adhesive Bonding Of Wood Materials. Wood Handbook: Wood As An Engineering Material. Madison, WI: USDA Forest Service, Forest Products Laboratory, 1999. General Technical Report FPL; GTR-113: Pages 9.1-9.24, 1999. 113.
66. Hunt, C.G., Et Al., Understanding Wood Bonds–Going Beyond What Meets The Eye: A Critical Review. Reviews Of Adhesion And Adhesives, 2018. 6(4): P. 369-440.
67. Ülker, O., Wood Adhesives And Bonding Theory. Adhesives, Intechopen, London, 2016: P. 271-288.
68. Stoeckel, F., J. Konnerth, And W. Gindl-Altmutter, Mechanical Properties Of Adhesives For Bonding Wood—A Review. International Journal Of Adhesion And Adhesives, 2013. 45: P. 32-41.
69. Schultz, J. And M. Nardin, Theories And Mechanisms Of Adhesion. Materials Engineering-New York-, 1999. 14: P. 1-26.
70. Gardner, D.J., Theories And Mechanisms Of Adhesion. Handbook Of Adhesive Technology, 2018: P. 3-18.
71. Norström, E., Hemicelluloses And Other Polysaccharides For Wood Adhesive Applications. 2018, Kungliga Tekniska Högskolan.
72. Baldan, A., Adhesion Phenomena In Bonded Joints. International Journal Of Adhesion And Adhesives, 2012. 38: P. 95-116.

73. Maeva, E., Et Al., Acoustical Methods For The Investigation Of Adhesively Bonded Structures: A Review. Canadian Journal Of Physics, 2004. 82(12): P. 981-1025.
74. Schultz, J. And M. Nardin, Theories And Mechanisms Of Adhesion. Hi: Handbook Of Adhesive Technology, Eds. A. Pizzi, And KL Mittal , 53-67. 2003, New York: Marcel Dekker.
75. Hale, K., The Potential Of Canola Protein For Bio-Based Wood Adhesives. 2013.
76. Gardner, D.J., Adhesion Mechanisms Of Durable Wood Adhesive Bonds. Characterization Of The Cellulosic Cell Wall, 2006: P. 254-265.
77. Ebnesajjad, S., Function Of Adhesives. Adhesive Technology Book, 2008. 2: P. 1-5.
78. Diwan, A.A., A.K.F. Hassan, And S.M. Thahab, Experimental Study Of Temperature Effect And Curing Time On The Shear Strength Of Adhesive Joints By Polyvinyl Pyrrolidone Pvp K30. Kufa Journal Of Engineering, 2017. 8(2): P. 53-66.
79. Ji, G., Study On Microstructure And Adhesion Property Of Electrospun Polymer Blends. 2015.
80. Teodorescu, M. And M. Bercea, Poly (Vinylpyrrolidone)–A Versatile Polymer For Biomedical And Beyond Medical Applications. Polymer-Plastics Technology And Engineering, 2015. 54(9): P. 923-943.
81. Tripathi, N., Studies On Poly (Lactic Acid) And Polysaccharide Gum Based Bionanocomposites For Adhesive And Gas Barrier Film Applications. 2016.
82. Gadhave, R.V., P.A. Mahanwar, And P.T. Gadekar, Study Of Cross-Linking Between Boric Acid And Different Types Of Polyvinyl Alcohol Adhesive. Open Journal Of Polymer Chemistry, 2019. 9(01): P. 16.
83. Gadhave, R.V., Et Al., Effect Of Addition Of Boric Acid On Thermo-Mechanical Properties Of Microcrystalline Cellulose/Polyvinyl Alcohol Blend And Applicability As Wood Adhesive. Journal Of Adhesion Science And Technology, 2020: P. 1-15.
84. Gadhave, R.V., Et Al., Effect Of Boric Acid On Poly Vinyl Alcohol-Tannin Blend And Its Application As Water-Based Wood Adhesive. Designed Monomers And Polymers, 2020. 23(1): P. 188-196.
85. Gadhave, R.V., Et Al., To Study The Effect Of Boric Acid Modification On Starch–Polyvinyl Alcohol Blend Wood Adhesive. Journal Of The Indian Academy Of Wood Science, 2018. 15(2): P. 190-198.
86. Li, N., Et Al., Effects Of Sodium Bisulfite On The Physicochemical And Adhesion Properties Of Canola Protein Fractions. Journal Of Polymers And The Environment, 2012. 20(4): P. 905-915.
87. Cheng, H., Et Al., Use Of Additives To Enhance The Properties Of Cottonseed Protein As Wood Adhesives. International Journal Of Adhesion And Adhesives, 2016. 68: P. 156-160.
88. Li, N., Et Al., Physicochemical Properties And Adhesion Performance Of Canola Protein Modified With Sodium Bisulfite. Journal Of The American Oil Chemists' Society, 2012. 89(5): P. 897-908.

89. Sit, N., S. Misra, And S.C. Deka, Physicochemical, Functional, Textural And Colour Characteristics Of Starches Isolated From Four Taro Cultivars Of North-E Ast India. Starch-Stärke, 2013. 65(11-12): P. 1011-1021.
90. Mark, A. And C. Mehltretter, Facile Preparation Of Starch Triacetates. Starch-Stärke, 1972. 24(3): P. 73-76.
91. Miladinov, V. And M. Hanna, Starch Esterification By Reactive Extrusion. Industrial Crops And Products, 2000. 11(1): P. 51-57.
92. Oladebeye, A., A. Oshodi, And A. Oladebeye, Physicochemical Properties Of Starches Of Sweet Potato (Ipomea Batata) And Red Cocoyam (Colocasia Esculenta) Cormels. Pakistan Journal Of Nutrition, 2009. 8(4): P. 313-315.
93. Tessema, A. And H. Admassu, Extraction And Characterization Of Starch From Anchote (Coccinia Abyssinica): Physico-Chemical, Functional, Morphological And Crystalline Properties. Journal Of Food Measurement And Characterization, 2021: P. 1-15.
94. Abegunde, O.K., Et Al., Physicochemical Characterization Of Sweet Potato Starches Popularly Used In Chinese Starch Industry. Food Hydrocolloids, 2013. 33(2): P. 169-177.
95. Desalegn, B.B., T. Teferra, And D. Buko, Physical And Proximate Characterization Of Anchote (Coccinia Abyssinica) Accessions Grown Under Hawassa And Wondo Genet Conditions, Southern Ethiopia. Food Science And Quality Management, 2015. 42: P. 62-74.
96. Xu, Y., Et Al., Morphological, Structural, And Thermal Properties Of Starch Nanocrystals Affected By Different Botanic Origins. Cereal Chemistry, 2014. 91(4): P. 383-388.
97. Pozo, C., Et Al., Study Of The Structural Order Of Native Starch Granules Using Combined FTIR And XRD Analysis. Journal Of Polymer Research, 2018. 25(12): P. 1-8.
98. Jane, J., Et Al., Amylose Contents And Amylopectin Branch Chain-Length Distributions Predominantly Affected The Pasting Properties Of Starch. Cereal Chemistry, 1999. 76: P. 629-637.
99. Chi, H., Et Al., Effect Of Acetylation On The Properties Of Corn Starch. Food Chemistry, 2008. 106(3): P. 923-928.
100. Abdullah, A., Et Al. Physical And Chemical Properties Of Corn, Cassava, And Potato Starchs. In IOP Conference Series: Earth And Environmental Science. 2018. IOP Publishing.
101. Tupa, M.V., Et Al., Organocatalytic Acetylation Of Starch: Effect Of Reaction Conditions On DS And Characterisation Of Esterified Granules. Food Chemistry, 2015. 170: P. 295-302.

102. Han, F., Et Al., Synthesis, Optimization And Characterization Of Acetylated Corn Starch With The High Degree Of Substitution. International Journal Of Biological Macromolecules, 2013. 59: P. 372-376.
103. Wang, X., Et Al., Research Advances In Chemical Modifications Of Starch For Hydrophobicity And Its Applications: A Review. Carbohydrate Polymers, 2020: P. 116292.
104. Otache, M., Et Al., Advances In The Modification Of Starch Via Esterification For Enhanced Properties. Journal Of Polymers And The Environment, 2021: P. 1-15.
105. Tupa, M., Et Al., Simple Organocatalytic Route For The Synthesis Of Starch Esters. Carbohydrate Polymers, 2013. 98(1): P. 349-357.
106. Garg, S. And A.K. Jana, Characterization And Evaluation Of Acylated Starch With Different Acyl Groups And Degrees Of Substitution. Carbohydrate Polymers, 2011. 83(4): P. 1623-1630.
107. Bartz, J., Et Al., Acetylation Of Barnyardgrass Starch With Acetic Anhydride Under Iodine Catalysis. Food Chemistry, 2015. 178: P. 236-242.
108. Mbougueng, P., Et Al., Influence Of Acetylation On Physicochemical, Functional And Thermal Properties Of Potato And Cassava Starches. Journal Of Food Engineering, 2012. 108(2): P. 320-326.
109. Machado, C.M., P. Benelli, And I.C. Tessaro, Effect Of Acetylated Starch On The Development Of Peanut Skin-Cassava Starch Foams. International Journal Of Biological Macromolecules, 2020. 165: P. 1706-1716.
110. El Halal, S.L.M., Et Al., Structure, Morphology And Functionality Of Acetylated And Oxidised Barley Starches. Food Chemistry, 2015. 168: P. 247-256.
111. Zhang, L., Et Al., Study On The Morphology, Crystalline Structure And Thermal Properties Of Yellow Ginger Starch Acetates With Different Degrees Of Substitution. Thermochimica Acta, 2009. 495(1-2): P. 57-62.
112. Colussi, R., Et Al., Structural, Morphological, And Physicochemical Properties Of Acetylated High-, Medium-, And Low-Amylose Rice Starches. Carbohydrate Polymers, 2014. 103: P. 405-413.
113. Bello-Pérez, L.A., Et Al., Effect Of Low And High Acetylation Degree In The Morphological, Physicochemical And Structural Characteristics Of Barley Starch. LWT-Food Science And Technology, 2010. 43(9): P. 1434-1440.
114. Xu, Y., V. Miladinov, And M.A. Hanna, Starch Acetate-Maleate Mixed Ester Synthesis And Characterization. Cereal Chemistry, 2005. 82(3): P. 336-340.
115. Luo, Z.-G. And Y.-C. Shi, Preparation Of Acetylated Waxy, Normal, And High-Amylose Maize Starches With Intermediate Degrees Of Substitution In Aqueous Solution And Their Properties. Journal Of Agricultural And Food Chemistry, 2012. 60(37): P. 9468-9475.
116. Khalil, M., A. Hashem, And A. Hebeish, Preparation And Characterization Of Starch Acetate. Starch-Stärke, 1995. 47(10): P. 394-398.

117. Gadhave, R.V., Et Al., Effect Of Addition Of Boric Acid On Thermo-Mechanical Properties Of Microcrystalline Cellulose/Polyvinyl Alcohol Blend And Applicability As Wood Adhesive. Journal Of Adhesion Science And Technology, 2021. 35(10): P. 1072-1086.
118. Alver, E., A.Ü. Metin, And H. Çiftçi, Synthesis And Characterization Of Chitosan/Polyvinylpyrrolidone/Zeolite Composite By Solution Blending Method. Journal Of Inorganic And Organometallic Polymers And Materials, 2014. 24(6): P. 1048-1054.
119. Othman, N., N.A. Azahari, And H. Ismail, Thermal Properties Of Polyvinyl Alcohol (PVOH)/Corn Starch Blend Film. Malaysian Polymer Journal, 2011. 6(6): P. 147-154.